Journal of
Marine Science and Engineering

MDPI

Article

Advanced Design of Naval Ship Propulsion Systems Utilizing Battery-Diesel Generator Hybrid Electric Propulsion Systems

Youngnam Park [1] and Heemoon Kim [2,*]

[1] Department of Marine System Engineering, Korea Maritime & Ocean University, 727 Taejong-ro, Busan 49112, Republic of Korea; youngnamy@hanmail.net
[2] Eco Friendly Propulsion System Technology Team, Korea Marine Equipment Research Institute, 28-36, Yusangongdan4-gil, Yangsan-si 50592, Republic of Korea
* Correspondence: hmkim@komeri.re.kr

Abstract: As advanced sensors and weapons require high power, naval vessels have increasingly adopted electric propulsion systems. This study aims to enhance the efficiency and operability of electric propulsion systems over traditional mechanical propulsion systems by analyzing the operational profiles of modern naval vessels. Consequently, a battery-integrated generator-based electric propulsion system was selected. Considering the purpose of the vessel, a specification selection procedure was developed, leading to the design of a hybrid electric propulsion system (comprising one battery and four generators). The power management control technique of the proposed propulsion system sets the operating modes (depending on the specific fuel oil consumption of the generators) to minimize fuel consumption based on the operating load. Additionally, load distribution control rules for the generators were designed to reduce energy consumption based on the load and battery state of charge. MATLAB/Simulink was used to evaluate the proposed system, with simulation results demonstrating that it maintained the same propulsion performance as existing systems while achieving a 12-ton (22%) reduction in fuel consumption. This improvement results in cost savings and reduced carbon dioxide emissions. These findings suggest that an efficient load-sharing controller can be implemented for various vessels equipped with electric propulsion systems, tailored to their operational profiles.

Keywords: optimal efficiency algorithm; power management system; energy management system; carbon dioxide emissions; battery management system

check for updates

Citation: Park, Y.; Kim, H. Advanced Design of Naval Ship Propulsion Systems Utilizing Battery-Diesel Generator Hybrid Electric Propulsion Systems. *J. Mar. Sci. Eng.* **2024**, *12*, 2034. https://doi.org/10.3390/jmse12112034

Academic Editors: Jian Shi, Bowen Xing and Gino Lim

Received: 10 October 2024
Revised: 2 November 2024
Accepted: 5 November 2024
Published: 10 November 2024

Copyright: © 2024 by the authors. Licensee MDPI, Basel, Switzerland. This article is an open access article distributed under the terms and conditions of the Creative Commons Attribution (CC BY) license (https://creativecommons.org/licenses/by/4.0/).

1. Introduction

1.1. Motivation

Globally, navies are increasingly adopting electric propulsion systems to meet the growing power demands of advanced sensors and weapons required for mission execution [1]. The Royal Navy pioneered this transition with the implementation of electric propulsion in its Type 23 Duke Class frigates [2]. Similarly, the United States Navy has employed an integrated power and energy system since the late 1990s to manage the highly dynamic loads and propulsion requirements of modern missions [3].

Since 2000, the Republic of Korea Navy has introduced hybrid ships that combine diesel generators (DGs), diesel engines, and gas turbines. These ships utilize electric propulsion systems with CODLOG (combined diesel-electric or gas turbine) and CODLOD (combined diesel-electric or diesel engine) configurations, specifically in Daegu-class frigates and Soyang-class logistics support ships [4]. However, to date, the Republic of Korea Navy has neither planned to adopt electric propulsion systems that employ batteries nor undertaken any related research.

The growing emphasis on environmental conservation in the civilian maritime sector has spurred rapid growth in the market for battery-powered electric propulsion ships.

Batteries are also expected to become increasingly price competitive [5]. Therefore, the Republic of Korea should consider adopting hybrid electric propulsion systems that incorporate battery technology.

1.2. Literature Review

The literature on ship propulsion systems can be broadly categorized into mechanical, electric, hybrid, and hybrid electric systems. Below is a summary presented in tabular form to highlight the key contributions and research focus areas:

Category	Research Focus	Key Contributions	References
Mechanical Propulsion Systems	Mechanical propulsion systems, being the most traditional, are still widely used in marine vessels due to their simplicity and relatively high reliability.	Operate most efficiently at 80% to 100% of the diesel engine's maximum speed, minimal conversion losses with reduced complexity, can combine diesel engines and gas turbines to enhance fuel efficiency and ensure optimal engine operation.	[6–9]
Electric Propulsion Systems	Electric propulsion systems were first introduced in the early 1900s but gained prominence in the mid-2000s due to concerns over oil supply reduction and tightening environmental regulations.	The DC distribution method provides motor efficiency, reduced fuel costs, weight and space savings, and simplified parallel generator connection; however, it requires PMS for power quality maintenance.	[10–13]
Hybrid Propulsion Systems	Hybrid propulsion systems operate electric motors in parallel with internal combustion engines. CODLOG systems employ electric motors during low-speed cruising, engines for high speed.	Achieve significant fuel savings during low-speed cruising, ideal for vessels that require extended low-speed operation and occasional high-speed bursts.	[14–17]
Hybrid Electric Propulsion Systems	The utilize two or more power sources, combining energy between generators and batteries.	Maximum energy efficiency achieved through bidirectional power transmission, reduction in maintenance costs compared with mechanical systems, emission reduction, use of batteries during significant power demands, providing improved generator operation.	[6,13,18–20]
Power Management Systems in Hybrid Systems	Hybrid electric propulsion vessels require PMSs to manage load sharing.	Techniques like droop control, rule-based control, optimization, DP, MPC, and ECMS are used. Droop control helps stabilize load sharing, while adaptive ECMS optimizes energy usage under dynamic conditions, achieving up to 10% fuel savings.	[21–42]

Mechanical propulsion systems, being the most traditional, are still widely used in marine vessels due to their simplicity and relatively high reliability, with diesel internal combustion engines serving as the primary power source [6]. These systems operate most efficiently at 80% to 100% of the maximum speed of the diesel engine [7]. With only three power conversion stages—the engine, gearbox, and propeller—they experience minimal conversion losses and reduced complexity, making them cost-effective [8]. Additionally, mechanical systems can combine diesel engines and gas turbines to enhance fuel efficiency and ensure optimal engine operation [9].

Electric propulsion systems were first introduced in the early 1900s but gained prominence in the mid-2000s due to concerns over global oil supply reduction and the tightening of environmental regulations [10]. In these systems, the direct current (DC) distribution method provides several advantages, including improved motor efficiency, reduced fuel costs, weight and space savings, decreased transmission losses, and simplified parallel connection of generators [11]. However, they are prone to significant degradation in power quality due to fluctuating power loads. To address this, a power management system (PMS) is employed to optimize the power load distribution [12]. Power control techniques are also essential for maintaining voltage and frequency stability, ensuring balanced load distribution among generators, and preventing blackouts [13].

Hybrid propulsion systems improve energy efficiency by minimizing fuel consumption, emissions, and costs while utilizing renewable energy. These systems operate electric motors in parallel with internal combustion engines [14]. They are powered by engines and electric motors connected to a propeller in either a parallel or series configuration. For example, CODLOG systems employ high-efficiency electric motors during low-speed cruising, while relying solely on the engine during high-speed operations. This configuration is particularly suitable for vessels that spend extended periods navigating at low speeds but require short bursts of high-speed operation [15,16]. Additionally, hybrid systems can achieve significant fuel savings during low-speed cruising [17].

Hybrid electric propulsion systems utilize two or more sources of power [6]. By combining and converting electrical energy between generators and batteries, maximum energy efficiency is achieved [18]. Power can be transmitted bidirectionally between mechanical and electrical components. For instance, the motor connected to the propeller can operate an electric drive during low-speed cruising, which reduces the risk of engine overload and lowers maintenance costs (compared with mechanical propulsion systems that require a gearbox for speed reduction) [13]. Notably, batteries supply power when a significant energy demand arises and are recharged when the generator is operating, enabling efficient generator operation, thereby reducing emissions and saving fuel [19]. As ship propulsion systems evolve, there is a strong focus on minimizing environmental pollutants and fuel consumption [20].

Hybrid electric propulsion vessels require PMSs to facilitate load sharing [21]. This study proposes a power management control technique that considers the power loads of naval vessels by reviewing existing power management methods. Representative power management control techniques include droop control [22], rule-based (RB) control [23], optimization-based control [24], dynamic programming (DP) [25], model predictive control [26], and an equivalent consumption minimization strategy (ECMS) [27].

Electric propulsion systems, whether using alternating current or DC distribution, require control techniques, with droop control being the most fundamental control method employed in both systems [6]. Droop control is crucial for maintaining stable operation in a distribution network when two or more generators are connected in parallel. It alleviates speed overshoot issues by lowering the governor speed setting as the load increases [28]. The speed droop regulates the load sharing of active power among the generators operating in parallel. When multiple engines are involved, the load-sharing ratio between the engines varies according to the speed droop settings of each engine. The voltage droop formula is derived by substituting the voltage for speed in the speed droop equation [29].

RB control relies on human expertise, predefined techniques, and set priorities [30]. It is easy to implement and does not require extensive computational effort [31]. However, it may not always provide optimal solutions and often requires significant tuning efforts, with its performance varying depending on the system topology [32,33]. In contrast, optimization-based techniques rely on analytical or numerical optimization algorithms [34]. Substantial research has been conducted on optimization-based PMSs and energy management systems (EMSs) [35].

DP is a well-known optimal method for addressing energy management problems in hybrid vehicles with a single battery [36]. The state of charge (SOC) of a battery is treated as a variable. The DP problem is represented by the diffusion of edges, which correspond to changes in the SOC and connect to the states in the next time step. Each edge reflects the battery current (changes in the SOC) and is associated with fuel consumption. The SOC can be sampled at each time step to correspond to the pure electric mode (maximum battery current), represented by one of the edges in the graph [37].

Recently, an ECMS [38] was applied to optimize load distribution in hybrid electric propulsion system ships, quantifying the equivalent fuel cost associated with battery energy usage [39] in hybrid vehicles [40]. To enhance the optimization performance of the ECMS, the equivalent factor must be continuously adjusted based on the changing operating conditions and the SOC of the energy storage device [41]. The application of a constant equivalent factor and an adaptive equivalent factor using ECMS has demonstrated that fuel consumption reductions can range from 5% to 10% compared with RB methods [42].

1.3. Research Gap

Previous studies have primarily focused on applying electric propulsion systems to civilian ships, considering power loads under full equipment operation. In contrast, this research aims to develop a hybrid electric propulsion system with battery integration, specifically tailored for naval vessels. It takes into account the variations in equipment operation based on mission requirements, reflecting changes in power loads.

While power control techniques in electric propulsion systems generally focus on optimizing generator operation in response to power load changes, this study goes further. It optimizes generator operation by incorporating battery operation within the range of power variations observed through an analysis of actual ship operational profiles.

Additionally, existing studies mainly concentrate on power management of hybrid electric propulsion systems. This research, however, presents a procedure for designing an electric propulsion system by determining battery and generator performance based on the operational profiles of actual ships, thereby facilitating the application of hybrid electric propulsion systems.

1.4. Contributions

This study proposes a method to convert naval vessels equipped with traditional mechanical propulsion systems into hybrid electric propulsion systems with integrated batteries. This approach aims to meet the increased power demands resulting from the modernization of naval equipment while achieving environmental protection and fuel savings.

The proposed hybrid electric propulsion system reflects power loads based on equipment operation under various naval mission requirements. It determines the performance of generators and batteries by analyzing power fluctuations observed in real operational profiles. Moreover, it presents an advanced power management control technique to optimize generator operation and enhance efficiency in hybrid propulsion systems.

1.5. Organization of the Study

This paper is organized as follows. Section 1 presents the background and necessity of this study, clarifying its objectives through an analysis of the gaps in existing research. Section 2 provides the theoretical basis and modeling methodology for transitioning from a conventional mechanical propulsion system to a battery-integrated hybrid electric propulsion system. In Section 3, the simulation results are quantitatively analyzed, followed by an in-depth discussion of the engineering implications and overall significance of the study in Section 4. Finally, Section 5 summarizes the findings, draws conclusions, and suggests directions for future research.

2. Materials and Methods

A naval vessel equipped with a mechanical propulsion system was selected as the target ship, with the battery-DG hybrid electric propulsion system modeled using a four-step process, as shown in Figure 1. First, the output and power loads of the vessel were analyzed to determine the system capacity. To minimize fuel oil consumption (FOC), the specific fuel oil consumption (SFOC) of the generator was set to 0%, 50%, 85%, and 100%, corresponding to different operating modes. Based on the system load, the conditions for the parallel operation of the four generators and rules for battery usage were established. The upper charging and lower discharge limits of the battery were defined to account for battery lifespan and ensure integrated operation. The generator-integrated battery system was verified using MATLAB (R2021b Update 7(9.11.0.2358333) 64-bit(win64) 16 August 2023)/Simulink R2021b to confirm its ability to handle system loads efficiently.

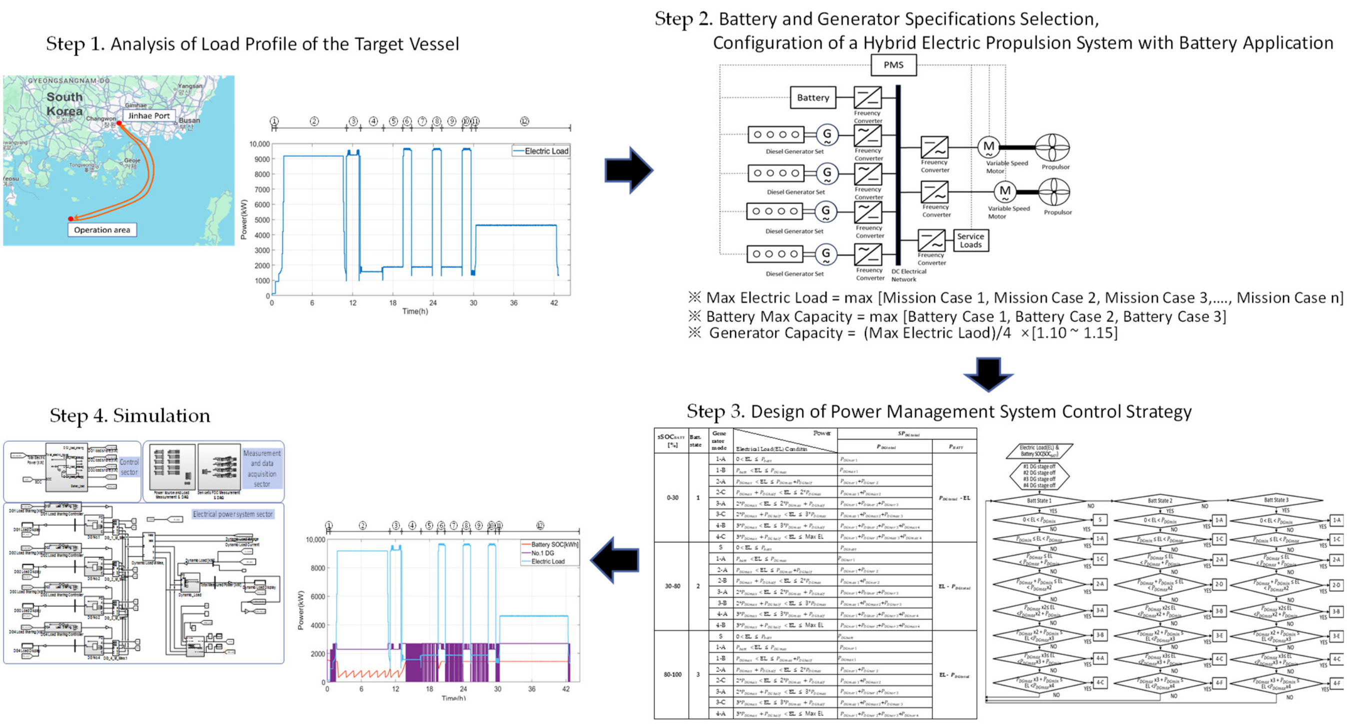

Figure 1. Design process of the proposed battery-DG hybrid electric propulsion system.

The steps for implementing the design are as follows:

Step 1: Analysis of the target vessel's propulsion load and power load.

Step 1-1: Selection of the target vessel.

This study implemented a battery-powered hybrid electric propulsion system using the Cheonghaejin-class ROK Navy vessel as the target ship. The primary mission of the target vessel is to provide support for search and rescue operations, such as personnel rescue and hull lifting during submarine distress situations. The specifications of the target vessel are presented in Table 1 [43].

Table 1. Specifications of the target vessel.

Category	General Characteristics
Displacement	3200 tones (3149 long tons) light
Size	Length: 102.8 m, beam: 16.4 m, draft: 4.6 m
Speed	18 kts (33 kmh), range: 17,594 km, 15 kts (27 kmh)
Main Equipment	Deep diving system, deep submersible rescue vehicle, remotely operated vehicle

Step 1-2: Load profile analysis.

To verify the reliability of the battery-powered hybrid electric propulsion system, scenarios were developed based on actual operational data from the target vessel, and simulations were conducted. The operational route of the vessel was selected to depart from Jinhae Port, conduct operations 10 m south of Yokjido, and return to the same location, as illustrated in Figure 2.

Figure 2. Map of voyage segments.

As listed in Table 2, the operational mode records for approximately 42 h (153,040 s) were extracted and transformed into load profiles for the simulation scenarios. The generator operating states were verified using MATLAB/Simulink, and the fuel consumption was calculated.

Table 2. Operating profile of the target vessel.

Day	Time	Description	Mission
1	08:30~09:00	① Departure preparation	At anchor
	09:00~19:03	② Movement to mission area	Normal navigation
	19:03~23:57	③ Operation of remotely operated vehicle	Underwater survey
	23:57~24:00	④ Operation of deep submersible rescue vehicle	Submarine rescue
2	00:00~03:29		
	03:29~06:30	⑤ Standby for saturation diving	Deep diving
	06:30~07:30	⑥ Saturation diving operations	
	07:30~10:56	⑦ Standby for saturation diving	
	10:56~11:56	⑧ Saturation diving operations	
	11:56~15:23	⑨ Standby for saturation diving	
	15:23~16:23	⑩ Saturation diving operations	
	16:23~17:07	⑪ Recovery operations	Recovery
	17:07~24:00	⑫ Return to port	Normal navigation
3	00:00~05:49		

Figure 3 shows the combined propulsion and power loads based on the operational modes. The following intervals are presented:

① Preparation for departure: Load during the mooring period while preparing for departure.
② Movement to work area: Load while moving from the base to the mission area.
③ Operation of underwater unmanned vehicle: Load during underwater exploration using an unmanned vehicle in a mission area.
④ Operation of deep-sea rescue submersible: Load during underwater exploration using a deep-sea rescue submersible in the mission area.
⑥, ⑦, and ⑨ Saturation diving wait period: Load while waiting in the mission area.
⑤, ⑧, and ⑩ Saturation diving operations: Load during saturation diving in the mission area.
⑪ Recovery operations: Load when recovering objects underwater.
⑫ Return to Jinhae Port: Load while moving from the mission area back to the base.

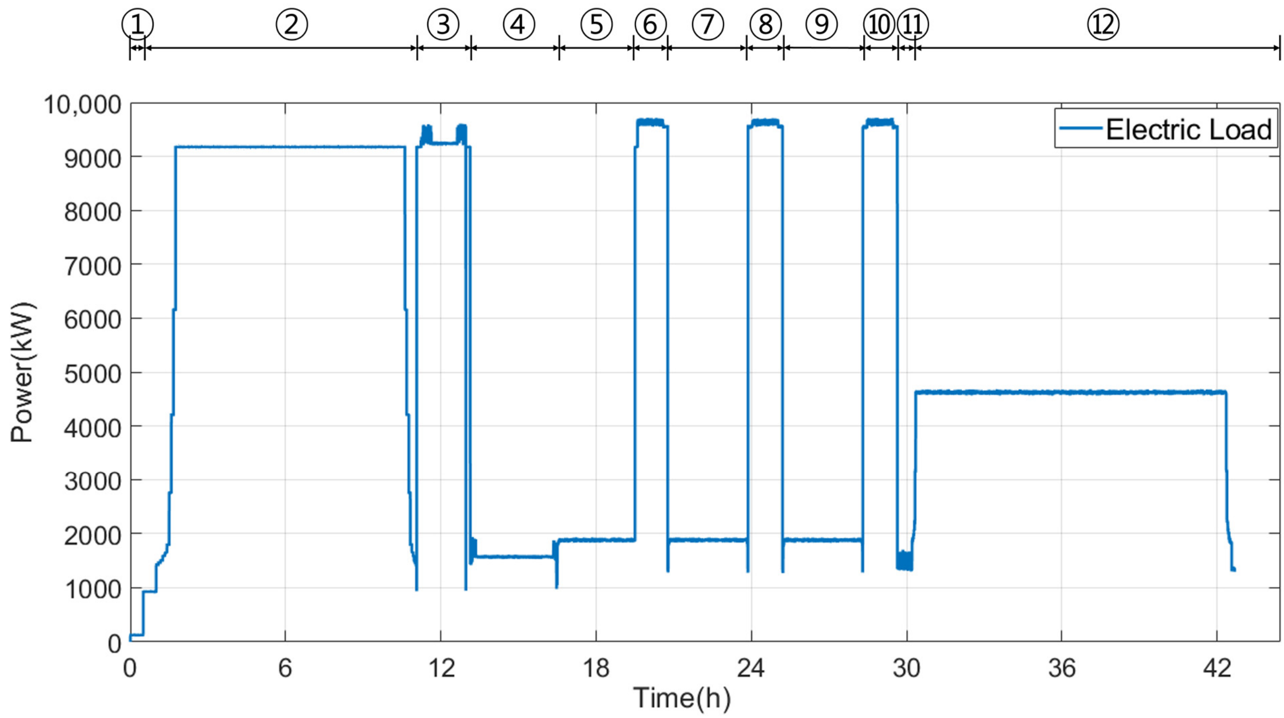

Figure 3. Combined propulsion and power loads on the operation modes according to load profile.

Data for these loads were recorded at 10 s intervals, with the assumption that the values remained constant between these intervals.

Step 1-3: Calculation of maximum power load.

The maximum power load, based on the voyage profile, is a crucial factor in designing the generator and battery capacities for a hybrid electric propulsion system. Naval vessels are equipped with various systems, including navigation equipment (such as radar and communication devices), weapon systems like guns and missiles (depending on the ship's mission), propulsion equipment for maneuvering, and support systems (comprising heating, cooling, and cooking devices). Table 3 presents the general classification and configuration of naval vessel equipment.

Table 3. General classification and configuration of equipment on naval vessels.

Category	Content
Navigation equipment	Navigation Radar, GPS, Wireless Communication, Satellite Communication, etc.
Armament	Guns, Missiles, Torpedoes, Anti-Air Radar, Electronic Warfare Equipment, etc.
Engine equipment	Engine, Generator, Seawater Pump, Freshwater Pump, etc.
Support equipment	Windlass, Capstan, Galley Equipment, Air Conditioning, Lighting, etc.

Naval vessels do not use all equipment simultaneously; instead, the equipment varies depending on the mission, such as general navigation, anti-surface warfare, anti-submarine warfare, and rescue operations. Table 4 provides examples of the equipment operations for different missions.

Table 4. Examples of operation equipment by mission.

Mission Case			Main Operational Equipment
1	At anchor (standby)		Some engine equipment, some support equipment
2	Normal navigation		Navigation equipment, engine equipment, some support equipment (e.g., galley)
3	Operations	Surface warfare	Normal navigation equipment + some armament (guns, anti-ship missiles, electronic warfare equipment)
4		Anti-air warfare	Normal navigation equipment + some armament (anti-air radar, guns, anti-air missiles, electronic warfare equipment)
5		Anti-submarine warfare	Normal navigation equipment + some armament (sonar, torpedoes)

The maximum power load is not simply the sum of the power loads required by all the equipment on the vessel. Instead, it must be calculated by analyzing the power loads of the equipment that operates according to the vessel's mission. Therefore, this study categorizes mission cases based on the tasks that the vessel will perform and compares the power requirements for each case to determine the maximum power load.

An analysis of the operation equipment and power load according to the target vessel's mission is presented in Table 5. During normal navigation, both navigation and engine equipment are operated, including the power load when the vessel moves at maximum speed. When performing deep-sea diving, the vessel requires a maximum power load of 9719 kW.

Table 5. Operation equipment and ELs by mission case.

Mission Case			Main Operational Equipment	Maximum Electric Load (kW)
1	At anchor (standby)		Some engine equipment, some support equipment	450
2	Normal navigation		Navigation equipment, engine equipment, some support equipment	9199
3	Operations	Deep diving	Navigation equipment, deep diving system	9719
4		Submarine rescue	Navigation equipment, seep submersible rescue vehicle	1079
5		Underwater survey	Navigation equipment, remotely operated vehicle	9619
6		Recovery	Navigation equipment, crane	960

Step 2: Determining the performance (capacity and quantity) of batteries and generators and configuration of the battery-DG hybrid electric propulsion system.

Step 2-1: Determining the number and performance (power output) of the generators.

The performance (power output) of the generator is determined by dividing the maximum power load by the number of generators. The considerations for selecting the number of generators are as follows:

① Stability of propulsion power operation.

A stable propulsion power must be maintained on the vessel. Generally, naval vessels utilize two propellers, which require two electric propulsion motors. Although both motors can be driven with a single generator, generator failure can hinder propulsion. To ensure stability in propulsion operations, one generator is allocated for each electric propulsion motor.

② Battery operated independently.

A separate generator is required to supply power for independent battery operations. The generator that powers the propulsion motors also provides power to the batteries. However, when determining the battery performance, it is important to consider that the power demand during docked standby situations is lower than the power required to operate the electric propulsion motors. Therefore, to reduce the shared power load, a generator is allocated for battery operation.

③ Ensuring the survivability of the vessel.

Unlike commercial vessels, naval vessels prioritize combat readiness by duplicating and spatially separating key equipment. Propulsion equipment is strategically placed on both the bow and the stern, as well as on the port and starboard sides, ensuring that the ship remains operational even if it sustains damage from enemy attacks. One generator is positioned on each side of the bow and stern, providing redundancy and enhancing the overall survivability of the vessel.

Considering factors ① and ②, three generators are required. However, based on the placement of generators on both the bow and the stern according to factor ③, this study proposes that the naval ship's electric propulsion system operates with four generators. The performance (power output) of one generator should be sufficient to share the maximum power load among the four generators. Typically, generators operate at their optimal SFOC at 80–85% of their maximum performance (power output) [44]. Therefore, this study proposes the application of a margin rate of 10–15%.

$$Generator\text{ capacity} = \frac{Max\ electric\ laod}{4} \times [1.10 \sim 1.15]$$

The number of generators and their performance are determined by applying the contents of items 1 and 3, which results in the operation of four generators. Each generator must be capable of handling a performance (power output) of 2429.7 kW. In this study, using the proposed formula, the generator performance was determined to be 2693 kW.

$$\begin{aligned} Generator\text{ capacity} &= \tfrac{Max\ electric\ laod}{4} \times [1.10 \sim 1.15] \\ &= \tfrac{9719\text{ kW}}{4} \times [1.10 \sim 1.15] = [2672.7 \sim 2794.2](\text{kW}) \end{aligned}$$

Considering the generator capacity required for the target vessel, this study proposes the use of a 2693 kW output DG produced by HYUNDAI-HiMSEN (HD Hyundai Heavy Industries Engine & Machinery (44032)1000, Bangeojinsumhwan-doro, Dong-gu, Ulsan, Republic of Korea) to configure the electric propulsion system. The detailed specifications are listed in Table 6.

The SFOC necessary for calculating the fuel consumption based on the load of the DG is presented in Table 7. These data are derived from the factory test operation report provided by the generator manufacturer during the construction of the target vessel.

As shown in Table 7, fuel consumption increases when the generator operates under low-load conditions compared with high-load operations. This indicates that fuel efficiency varies with load, revealing a significant difference in efficiency between low-load and high-load operations. While the variation at load levels above 50% is small, the efficiency decreases sharply when the generator is operated at loads below 50%.

Table 6. Specifications of the HYUNDAI-HiMSEN generator.

Maker	HYUNDAI-HiMSEN
Type	9H25/33M
Engine power [kW]	2835
Generator power [kW]	2693
Engine speed [rpm]	900
Engine set [sets]	4

Table 7. SFOC data for the designated HYUNDAI-HiMSEN generator.

Engine power [%]	25	50	75	85	100	110
SFOC [g/kWh]	214	190	184	183.3	183	184

Step 2-2: Determining battery performance (power capacity).

In an electric propulsion system, the battery serves three main purposes: first, to drive the propulsion motor to provide thrust; second, to supply the power required for vessel operations; and third, to provide a temporary power supply in the event of a generator failure [45].

The battery performance can be determined based on its operational purpose in naval vessels, as shown in Table 8. In this study, the battery serves three main functions: First, it supplies the power necessary for the ship's operations during anchorage (case 1). Second, it is utilized as the primary propulsion power during low-speed navigation (case 2). Third, it acts as a temporary power supply in the event of generator failure during any mission (case 3).

Table 8. Function description according to battery cases.

Battery Case		Description
1	At anchor (standby)	Power in mission case 1
2	Low-speed navigation	Power during low-speed in mission case 2
3	Uninterruptible power supply	Power required for navigation equipment operation during the time needed to activate an alternate generator in case of generator failure

Therefore, among the three cases, the maximum power capacity of the battery is determined by the capacity to handle the maximum power load.

The power requirements for the battery in the target vessel are listed in Table 9. In this study, a battery capacity of 1600 kWh was required to handle a power load of 1550 kWh during slow navigation.

Table 9. Required electric capacity for battery according to case type.

Battery Case		Maximum Required Electric Capacity (kWh)
1	At anchor (Standby)	450
2	Low-speed navigation	1550
3	Uninterruptible power supply	350

Step 2-3: Battery-DG hybrid electric propulsion system.

By selecting the specifications for the battery and generator, a hybrid electric propulsion system was configured as Figure 4, consisting of one battery and four generators (as illustrated). The PMS monitored one battery, four generators, two electric propulsion motors, and the power load of the vessel. The PMS tracks both service and motor loads by controlling the operation of the battery and generators to satisfy the power load requirements of the vessel. This study proposes a PMS that controls the operation of generators according to the battery's SOC to effectively manage the power load of the vessel.

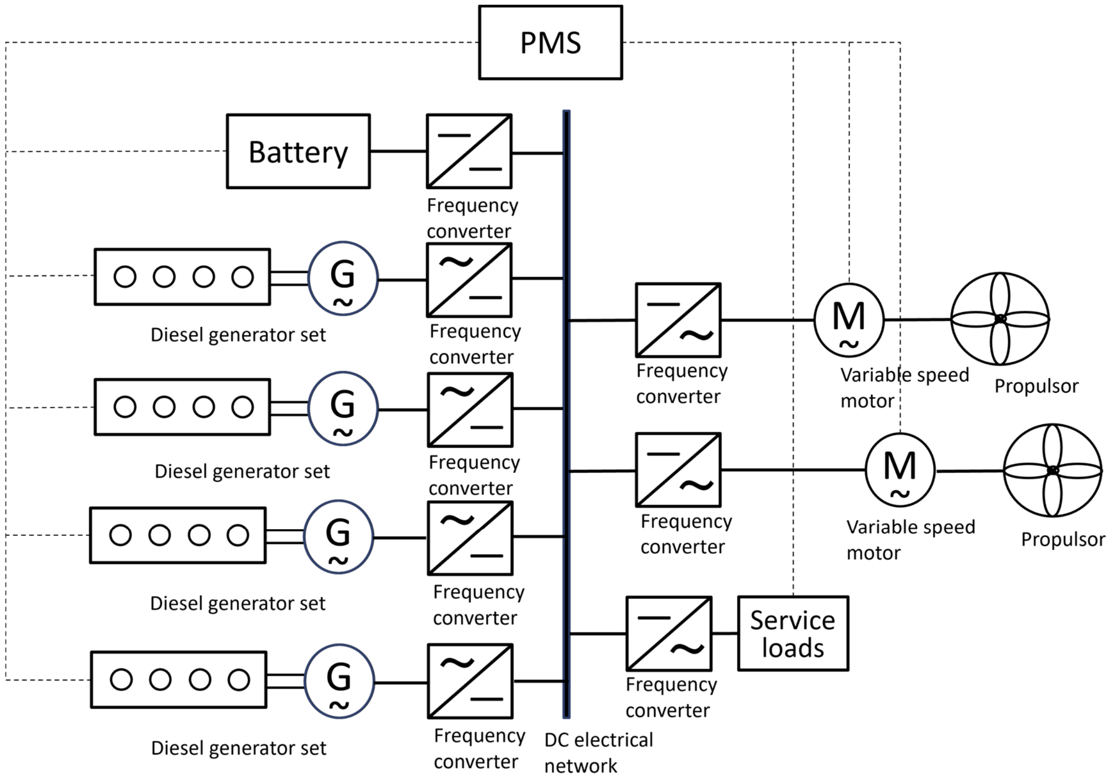

Figure 4. Configuration of battery-DG hybrid system using PMS.

Step 3: Design of PMS control method.

Step 3-1: Power management control equation.

The operating mode was established considering the generator output and the SFOC, with the PMS configured to ensure that the generator output meets the total EL of the vessel based on the overall power demand and the battery's SOC.

The total EL of a vessel can be expressed as the sum of the service and motor loads, as shown in Equation (1).

$$\text{EL} = \text{Service Load} + \text{Motor Load} \quad (1)$$

$\boldsymbol{SOC_{batt}}$ represents the SOC of the battery.

The power balance between each generator and the battery is the sum of the outputs of n generators and the battery capacity (which equals the total EL), as shown in Equation (2).

$$SP_{DGtotal} = P_{DGtotal} + P_{BATT} = \sum_{i=1}^{n} P_{DGi} + P_{BATT} \quad (2)$$

$SP_{DGtotal}$: total output (kW)of ship;
$P_{DGtotal}$: total output (kW) of DGs;
P_{BATT}: output (kW) of battery;
$P_{DG\bullet i}$: output (kW) of DG.

To set the generator output based on the ship's EL and the battery's SOC ($\boldsymbol{SOC_{batt}}$), the operating modes were established using output levels corresponding to the SFOC of the DGs (as listed in Table 7). This approach ensures that the generators operate efficiently and effectively to meet varying power demands while considering $\boldsymbol{SOC_{batt}}$.

The operating modes for DGs are defined as follows:

$$DG_{stop} : 0\%, DG_{min} : 50\%, DG_{opt} : 85\%, DG_{max} : 100\%$$

$P_{DGtotal}$ is the sum of the outputs for each mode, corresponding to DG_{stop}, DG_{opt}, and DG_{max} for the n generators shown in Equation (3).

$$P_{DGtotal} = \sum_{i=1}^{n} P_{DGmode} \cdot i \quad (3)$$

FOC (C_{fuel}) is calculated as the sum of the SFOCs of the generator per hour, as expressed in Equation (4).

$$C_{fuel} = \int_{t0}^{t} mf \sum_{i=1}^{n} (t, \sigma_{DG \cdot iSFOC}) \quad (4)$$

C_{fuel}: total fuel consumption of ship;
mf: fuel rate;
$\sigma_{DG \cdot iSFOC}$: SFOC variation at time t.
Step 3-2: Power management control algorithm.

The power management control technique proposed in this study was designed to minimize fuel consumption by adjusting the generator operation based on the ship's EL and SOC_{batt}. The operating loads and outputs of each generator mode are detailed in Table 10.

Table 10. Generator modes based on operating loads and outputs.

Electric Load [%]	Electric Load (kW)	Generator Mode	
		Content	Notation
0	0	0	S
50	1347	DG_{min}	1-A
85	2289	DG_{opt}	1-B
100	2693	DG_{max}	1-C
150	4040	DG_{max} + DG_{min}	2-A
170	4578	DG_{opt} + DG_{opt}	2-B
185	4982	DG_{max} + DG_{opt} (=DG_{min} + DG_{min} + DG_{opt})	2-C
200	5386	DG_{max} + DG_{max} (=DG_{min} + DG_{min} + DG_{min} + DG_{min})	2-D
220	5925	DG_{opt} + DG_{opt} + DG_{min}	3-A
235	6329	DG_{min} + DG_{min} + DG_{min} + DG_{opt}	omit1)
255	6867	DG_{opt} + DG_{opt} + DG_{opt}	3-B
270	7271	DG_{opt} + DG_{opt} + DG_{max} (=DG_{min} + DG_{min} + DG_{opt}+DG_{opt})	3-C
285	7675	DG_{opt} + DG_{max} + DG_{max}	3-D
300	8079	DG_{max} + DG_{max} + DG_{max}	3-E
305	8214	DG_{min} + DG_{opt} + DG_{opt} + DG_{opt}	4-A
340	9156	DG_{opt} + DG_{opt} + DG_{opt} + DG_{opt}	4-B
355	9560	DG_{opt} + DG_{opt} + DG_{opt} + DG_{max}	4-C

Table 10. *Cont.*

Electric Load [%]	Electric Load (kW)	Generator Mode	
		Content	Notation
370	9964	$DG_{opt} + DG_{opt} + DG_{max} + DG_{max}$	4-D
385	10,368	$DG_{opt} + DG_{max} + DG_{max} + DG_{max}$	4-E
400	10,772	$DG_{max} + DG_{max} + DG_{max} + DG_{max}$	4-F

When the EL of the ship was 50%, the power output was 1347 kW, with the operating mode represented as DG_{min} (1-A). When the EL reached 185%, the power output was 4982 kW, with the operating mode represented as $DG_{max} + DG_{opt}$, which is equivalent to $DG_{min} + DG_{min} + DG_{min} + DG_{min}$, denoted as 2-C.

In this study, to ensure battery protection, the following SOC management strategy was applied [46]: In the range of 100% ≥ $\boldsymbol{SOC_{batt}}$ ≥ 90%, only discharging occurs; when 90% > $\boldsymbol{SOC_{batt}}$ ≥ 20%, both charging and discharging are allowed, and for 20% > $\boldsymbol{SOC_{batt}}$ ≥ 0%, only charging is permitted. Table 11 details the amount of power that the generator must supply based on the generator operating modes and $\boldsymbol{SOC_{batt}}$.

Table 11. Generator operating modes based on ELs and battery SOC.

Electric Load [%]	Electric Power (kW)	Battery SOC (%/kWh)										
		100	**90**	**80**	**70**	**60**	**50**	**40**	**30**	**20**	**10**	**0**
		1600	**1440**	**1280**	**1120**	**960**	**800**	**640**	**480**	**320**	**160**	**0**
400	10,772	9172	9332	9492	9652	9812	9972	10,132	10,292	10,452	10,772	10,772
Generator mode		4-C	4-C	4-C	4-D	4-D	4-E	4-E	4-E	4-F	4-F	4-F
385	10,368	8768	8928	9088	9248	9408	9568	9728	9888	10,048	10,368	10,368
Generator mode		4-B	4-B	4-B	4-C	4-C	4-D	4-D	4-D	4-E	4-E	4-E
370	9964	8364	8524	8684	8844	9004	9164	9324	9484	9644	9964	9964
Generator mode		4-B	4-B	4-B	4-B	4-B	4-C	4-C	4-C	4-D	4-D	4-D
355	9560	7960	8120	8280	8440	8600	8760	8920	9080	9240	9560	9560
Generator mode		3-E	4-A	4-B	4-B	4-B	4-B	4-B	4-B	4-C	4-C	4-C
340	9156	7556	7716	7876	8036	8196	8356	8516	8676	8836	9156	9156
Generator mode		3-D	3-E	3-E	3-E	4-A	4-B	4-B	4-B	4-B	4-B	4-B
305	8214	6614	6774	6934	7094	7254	7414	7574	7734	7894	8214	8214
Generator mode		3-B	3-B	3-C	3-C	3-C	3-D	3-D	3-E	3-E	4-A	4-A
300	8079	6479	6639	6799	6959	7119	7279	7439	7599	7759	8079	8079
Generator mode		3-B	3-B	3-B	3-C	3-C	3-D	3-D	3-D	3-E	3-E	3-E
285	7675	6075	6235	6395	6555	6715	6875	7035	7195	7355	7675	7675
Generator mode		3-B	3-B	3-B	3-B	3-B	3-D	3-D	3-D	3-D	3-D	3-D
270	7271	5671	5831	5991	6151	6311	6471	6631	6791	6951	7271	7271
Generator mode		3-A	3-A	3-B	3-B	3-B	3-B	3-B	3-B	3-C	3-C	3-C
255	6867	5267	5427	5587	5747	5907	6067	6227	6387	6547	6867	6867
Generator mode		2-D	3-A	3-A	3-A	3-A	3-B	3-B	3-B	3-B	3-B	3-B
220	5925	4325	4485	4645	4805	4965	5125	5285	5445	5605	5925	5925
Generator mode		2-B	2-B	2-C	2-C	2-C	2-D	2-D	2-D	3-A	3-A	3-A

Table 11. *Cont.*

Electric Load [%]	Electric Power (kW)	Battery SOC (%/kWh)										
		100	**90**	**80**	**70**	**60**	**50**	**40**	**30**	**20**	**10**	**0**
		1600	**1440**	**1280**	**1120**	**960**	**800**	**640**	**480**	**320**	**160**	**0**
200	5386	3786	3946	4106	4266	4426	4586	4746	4906	5066	5386	5386
Generator mode		2-A	2-A	2-B	2-B	2-B	2-C	2-C	2-C	2-D	2-D	2-D
185	4982	3382	3542	3702	3862	4022	4182	4342	4502	4662	4982	4982
Generator mode		2-A	2-A	2-A	2-A	2-A	2-B	2-B	2-B	2-C	2-C	2-C
170	4578	2978	3138	3298	3458	3618	3778	3938	4098	4258	4578	4578
Generator mode		2-A	2-A	2-A	2-A	2-A	2-A	2-A	2-B	2-B	2-B	2-B
150	4040	2440	2600	2760	2920	3080	3240	3400	3560	3720	4040	4040
Generator mode		1-C	1-C	2-A	2-A	2-A	2-A	2-A	2-A	2-A	2-A	2-A
100	2693	1093	1253	1413	1573	1733	1893	2053	2213	2373	2693	2693
Generator mode		1-A	1-A	1-B	1-B	1-B	1-B	1-B	1-B	1-C	1-C	1-C
85	2289	689	849	1009	1169	1329	1489	1649	1809	1969	2289	2289
Generator mode		1-A	1-A	1-A	1-A	1-A	1-B	1-B	1-B	1-B	1-B	1-B
50	1347	−254	−94	67	227	387	547	707	867	1027	1347	1347
Generator mode		S	S	1-A	1-A	1-A	1-A	1-A	1-A	1-A	1-A	1-A
0	0	−1600	−1440	−1280	−1120	−960	−800	−640	−480	−320	0	0
Generator mode		S	S	S	S	S	S	S	S	S	S	S

For instance, when the ship's power load is at 50% and SOC_{batt} is 90%, the generator operates in mode "*S*" (standby). This indicates that the generator is not running and that the battery alone supplies the required power. In this scenario, if the ship's power demand is 1347 kW (which is 50% of the generator's capacity), the battery, with an SOC_{batt} of 90%, provides 1440 kW, leaving a surplus of 94 kW.

In contrast, when the power load is 50% and SOC_{batt} is 50%, the generator operates in mode 1-A, where Generator #1 runs at DG_{min}. Initially, the battery supports the ship's required power load, supplying 800 kW, and the generator compensates for the remaining 547 kW to meet the total load of 1347 kW.

Similarly, in the same interval, if SOC_{batt} is 10%, the generator remains in mode 1-A, with Generator #1 still operating at DG_{min}. However, since the battery is in a discharging state and cannot meet the required power load of the ship, the generator must supply the entire 1347 kW of power.

Table 12 lists the battery charging status (Batt. state) according to SOC_{batt} and the generator operating modes. This is based on the vessel's power load (EL) and the total power output ($SP_{DGtotal}$). The intervals for SOC_{batt} are defined as follows: The range of 100% $\geq SOC_{batt} \geq$ 90% indicates battery charging, 90% > $SOC_{batt} \geq$ 20% allows for either battery charging or discharging, and 20% > $SOC_{batt} \geq$ 0% facilitates charging only. The generators are controlled based on these EL intervals.

When SOC_{batt} falls below 20%, the battery is charged until it reaches an SOC_{batt} of 50%. During this process, the number of operating generators is adjusted to meet the vessel's required power load (EL). The operating modes of the generators change based on the required power load, and the total power output of the generators ($P_{DGtotal}$) is utilized to satisfy this load. Any excess power ($\mathbf{EL} - P_{DGtotal}$) is returned to the battery. Since the battery is in a discharged state, P_{BATT} will have a negative value.

Table 12. Proposed load sharing rules.

Batt. State	SOC_{batt}	**Electrical Load (EL) Condition**	**Generator Mode**	$SP_{DGtotal}$				
				$P_{DGtotal}$				P_{BATT}
				P_{DG1}	P_{DG2}	P_{DG3}	P_{DG4}	
1	100 ~ 90	$0 \leq$ EL < P_{DGmin}	S	0	-	-	-	EL − $P_{DGtotal}$
		$P_{DGmin} \leq$ EL < P_{DGmax}	1-A	DG_{min}	-	-	-	
		$P_{DGmax} \leq$ EL < $P_{DGmax} + P_{DGmin}$	1-C	DG_{max}	-	-	-	
		$P_{DGmax} + P_{DGmin} \leq$ EL < $P_{DGmax} \times 2$	2-A	DG_{max}	DG_{min}	-	-	
		$P_{DGmax} \times 2 \leq$ EL < $P_{DGmax} \times 2$ + P_{DGmin}	3-A	DG_{opt}	DG_{opt}	DG_{min}	-	
		$P_{DGmax} \times 2$ + $P_{DGmin} \leq$ EL < $P_{DGmax} \times 3$	3-B	DG_{opt}	DG_{opt}	DG_{opt}	-	
		$P_{DGmax} \times 3 \leq$ EL < $P_{DGmax} \times 3$ $+P_{DGmin}$	4-A	DG_{opt}	DG_{opt}	DG_{opt}	DG_{min}	
		$P_{DGmax} \times 3 + P_{DGmin} \leq$ EL < $P_{DGmax} \times 4$	4-C	DG_{opt}	DG_{opt}	DG_{opt}	DG_{max}	
2	90 ~ 20	$0 \leq$ EL < P_{DGmin}	1-A	DG_{opt}	-	-	-	EL − $P_{DGtotal}$
		$P_{DGmin} \leq$ EL < P_{DGmax}	1-C	DG_{max}	-	-	-	
		$P_{DGmax} \leq$ EL < $P_{DGmax} + P_{DGmin}$	2-A	DG_{max}	DG_{min}	-	-	
		$P_{DGmax} + P_{DGmin} \leq$ EL < $P_{DGmax} \times 2$	2-D	DG_{max}	DG_{max}	-	-	
		$P_{DGmax} \times 2 \leq$ EL < $P_{DGmax} \times 2$ $+P_{DGmin}$	3-B	DG_{opt}	DG_{opt}	DG_{opt}	-	
		$P_{DGmax} \times 2 + P_{DGmin} \leq$ EL < $P_{DGmax} \times 3$	3-E	DG_{max}	DG_{max}	DG_{max}	-	
		$P_{DGmax} \times 3 \leq$ EL < $P_{DGmax} \times 3$ $+P_{DGmin}$	4-C	DG_{opt}	DG_{opt}	DG_{opt}	DG_{max}	
		$P_{DGmax} \times 3 + P_{DGmin} \leq$ EL < $P_{DGmax} \times 4$	4-F	DG_{max}	DG_{max}	DG_{max}	DG_{max}	
3	20 ~ 0	$0 \leq$ EL < P_{DGmin}	1-A	DG_{opt}	-	-	-	EL − $P_{DGtotal}$
		$P_{DGmin} \leq$ EL < P_{DGmax}	1-C	DG_{max}	-	-	-	
		$P_{DGmax} \leq$ EL < $P_{DGmax} + P_{DGmin}$	2-A	DG_{max}	DG_{min}	-	-	
		$P_{DGmax} + P_{DGmin} \leq$ EL < $P_{DGmax} \times 2$	2-D	DG_{max}	DG_{max}	-	-	
		$P_{DGmax} \times 2 \leq$ EL < $P_{DGmax} \times 2$ $+P_{DGmin}$	3-B	DG_{opt}	DG_{opt}	DG_{opt}	-	
		$P_{DGmax} \times 2 + P_{DGmin} \leq$ EL < $P_{DGmax} \times 3$	3-E	DG_{max}	DG_{max}	DG_{max}	-	
		$P_{DGmax} \times 3 \leq$ EL < $P_{DGmax} \times 3$ $+P_{DGmin}$	4-C	DG_{opt}	DG_{opt}	DG_{opt}	DG_{max}	
		$P_{DGmax} \times 3 + P_{DGmin} \leq$ EL < $P_{DGmax} \times 4$	4-F	DG_{max}	DG_{max}	DG_{max}	DG_{max}	

As illustrated in Table 12, when EL = 2 × $\boldsymbol{P_{DGmax}}$, the generator operating mode is 3-A. In this mode, Generator #1 operates in DG_{opt}, Generator #2 in DG_{opt}, and Generator #3 in DG_{opt} The power balance between each of the ship's generators and the battery is expressed as follows:

$$SP_{DGtotal} = P_{DGtotal} + P_{BATT} = P_{DG1} + P_{DG2} + P_{DG3} - (\text{EL} - P_{DGtotal})$$
$$= DG_{opt} + DG_{opt} + DG_{opt} - (\text{EL} - P_{DGtotal})$$

When SOC_{batt} is between 20% and 90%, the rules allow for both charging and discharging across all ranges (according to the EL). The number of operating generators is adjusted to satisfy the power demand of the ship. Depending on the EL, the generator operating mode changes, and the power demand is satisfied through the combined output of the generators ($\boldsymbol{P_{DGtotal}}$) and battery power ($\mathbf{EL} - \boldsymbol{P_{DGtotal}}$). The remaining power is then used to charge the battery. During this process, the battery may either charge or discharge, resulting in $\boldsymbol{P_{BATT}}$ having either a positive or negative value.

For example, when EL = 2 × $\boldsymbol{P_{DGmax}}$ in Table 12, the generator operating mode is 3-B. In this mode, Generator #1 operates in DG_{opt}, Generator #2 in DG_{opt}, and Generator #3 in DG_{opt}. The power balance between each generator and the battery of the ship is represented as follows:

$$SP_{DGtotal} = P_{DGtotal} + P_{BATT} = P_{DG1} + P_{DG2} + P_{DG3} - (\text{EL} - P_{DGtotal})$$
$$= DG_{opt} + DG_{opt} + DG_{opt} - (\text{EL} - P_{DGtotal})$$

When SOC_{batt} exceeds 90%, the battery discharges until SOC_{batt} drops below 90%. The number of operating generators is adjusted to satisfy the EL. The operating mode of the generator changes according to the EL of the vessel. The total load is satisfied through the combined output of the generators ($\boldsymbol{P_{DGtotal}}$) and battery power ($\mathbf{EL} - \boldsymbol{P_{DGtotal}}$). The remaining power is used to charge the battery. In this case, because the battery is charging, $\boldsymbol{P_{BATT}}$ has a positive value.

As noted when EL = 2 × $\boldsymbol{P_{DGmax}}$ in Table 12, the generator operating mode is 3-B. Here, Generator #1 operates in DG_{opt}, Generator #2 in DG_{opt}, and Generator #3 in DG_{opt}. The power balance of each generator and the battery of the ship is expressed as follows:

$$SP_{DGtotal} = P_{DGtotal} + P_{BATT} = P_{DG1} + P_{DG2} + P_{DG3} - (\text{EL} - P_{DGtotal})$$
$$= DG_{opt} + DG_{opt} + DG_{opt} - (\text{EL} - P_{DGtotal})$$

Figure 5 illustrates a flowchart detailing the charging and discharging modes (Batt. state) based on $\boldsymbol{SOC_{batt}}$ and the generator operating mode (depending on the ship's EL). Starting from a state wherein the ship's generators are inoperative, the battery state (Batt. state) progresses according to $\boldsymbol{SOC_{batt}}$. It moves through distinct states: discharge only (Batt. state 1), charging or discharging (Batt. state 2), and charging only (Batt. state 3). In each battery state, the generator operating mode is adjusted to satisfy the EL of the ship. The system continuously monitors changes in the EL and $\boldsymbol{SOC_{batt}}$ to ensure it operates in the appropriate generator mode.

Step 4: Simulation.

To validate the proposed hybrid electric propulsion system, modeling was performed using MATLAB/Simulink, incorporating the previously analyzed vessel operation profiles. Figure 6 shows the overall configuration of the proposed hybrid electric propulsion system. It is composed of one battery (1600 kW) and four generators (2693 kW), with their performances determined based on an analysis of the power load requirement of the target vessel.

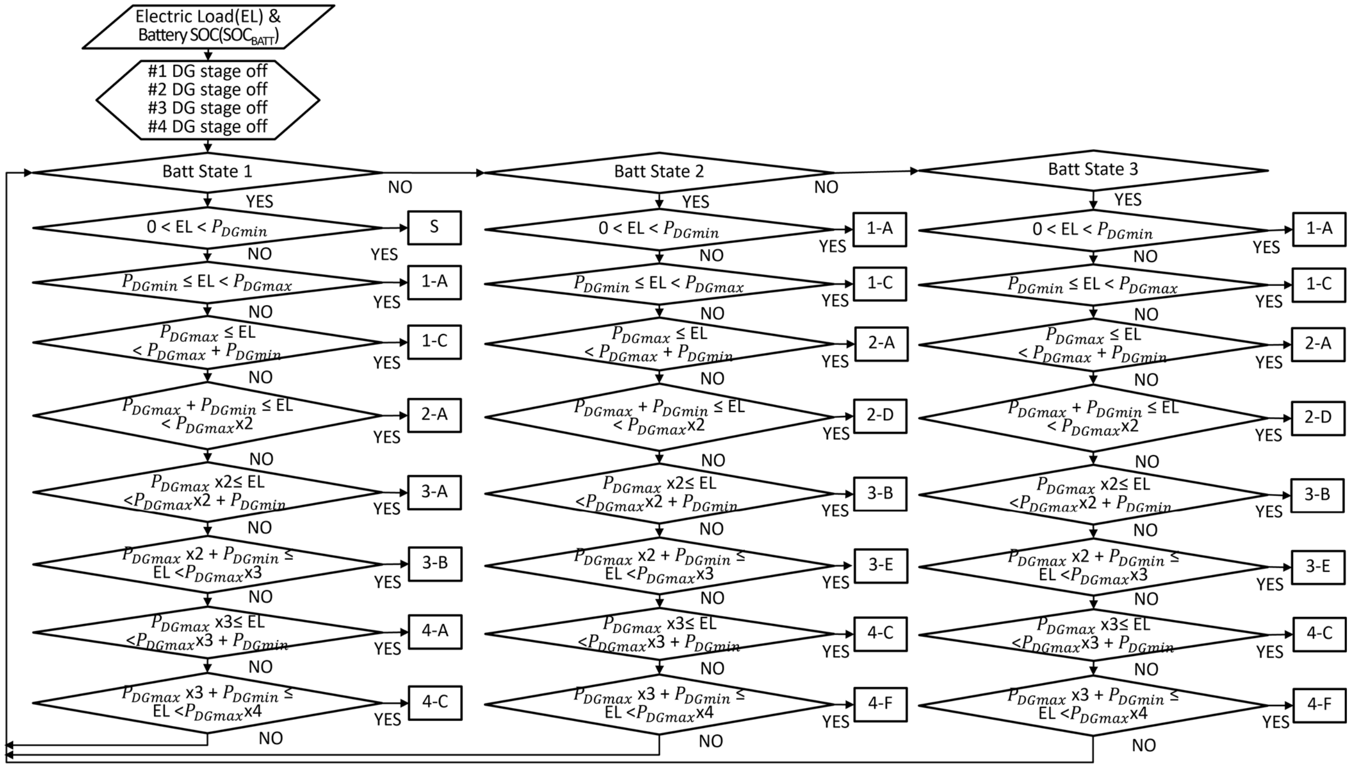

Figure 5. Block diagram of the operation sequence for the proposed hybrid system.

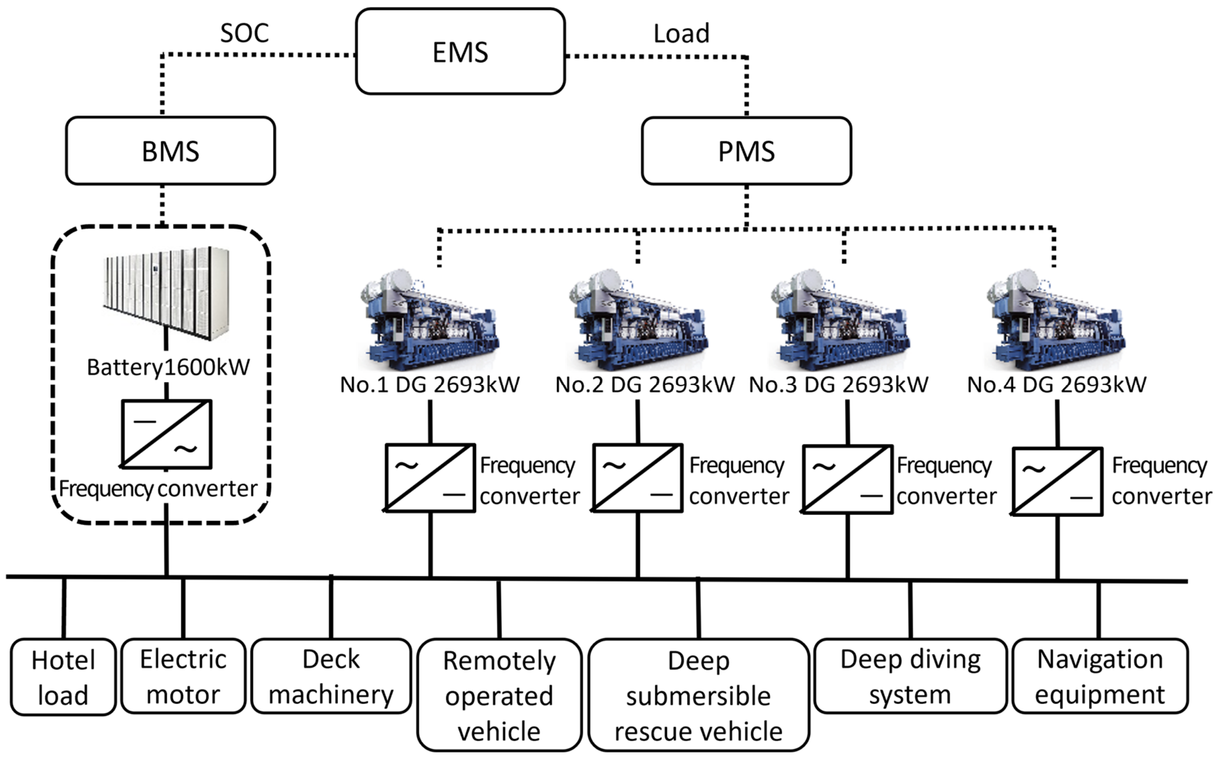

Figure 6. Overall configuration of the proposed hybrid electric propulsion system.

Figure 7 illustrates the modeling of the proposed hybrid electric propulsion system using MATLAB/Simulink R2021b software (R2021b Update 7(9.11.0.2358333) 64-bit(win64) 16 August 2023). The characteristics of the selected generator's FOC were integrated to facilitate data extraction, including generator output, FOC, voltage, and current across different generator operation modes. To verify the operational status of the power management control method based on the vessel's EL and $\boldsymbol{SOC_{batt}}$, an initial SOC value of the battery was established. The control sector is responsible for power management control, the measurement and data acquisition sector collects data, and the electrical power system sector implements the generators and power loads.

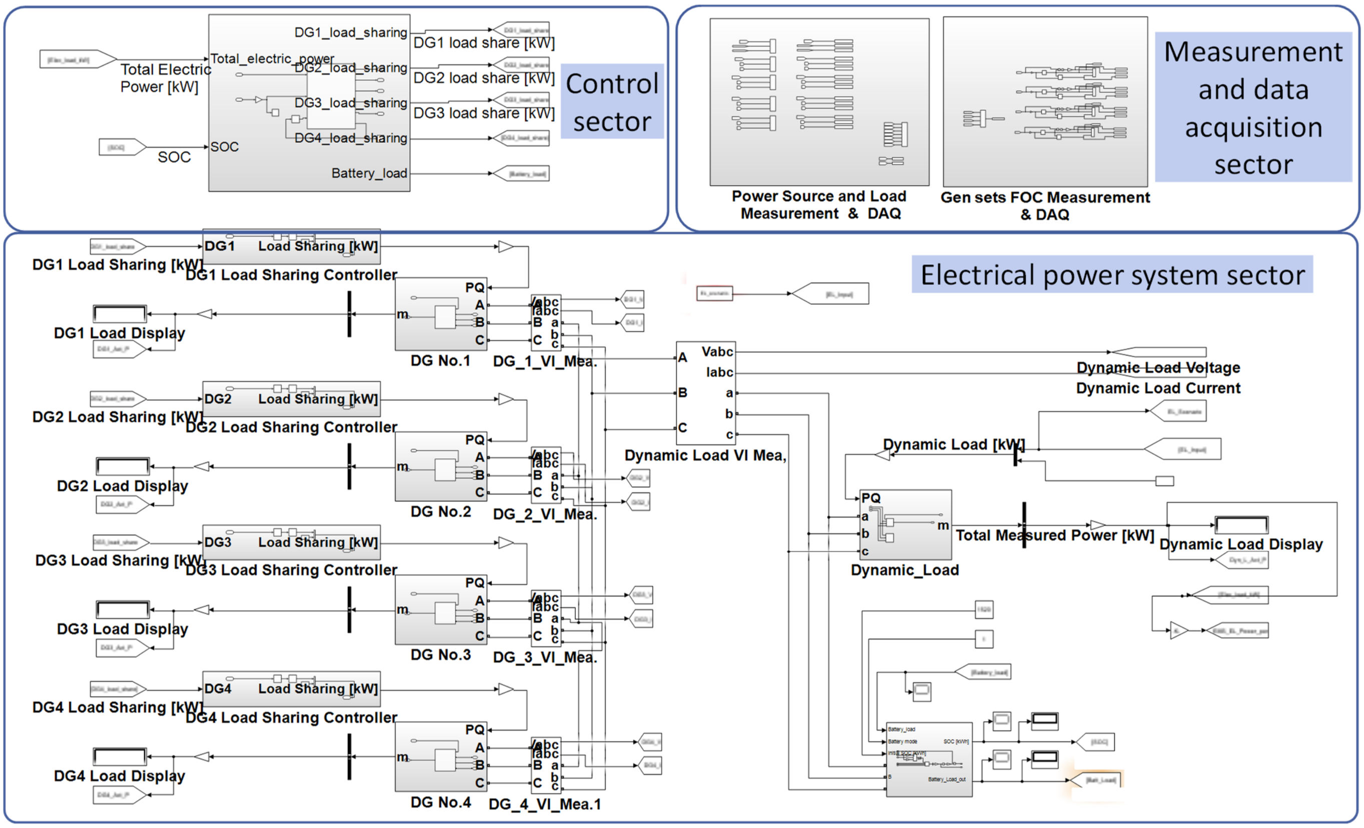

Figure 7. Model of the proposed hybrid electric propulsion system.

3. Results

The power load distribution status for each generator operation mode was verified based on the vessel's power load (EL) and SOC_{batt} in the ship's operation profile. The initial value of SOC_{batt} was set to 95%, within the range of 100% $\geq SOC_{batt} >$ 90%, corresponding to 1520 kW. The charging and discharging conditions were observed based on SOC_{batt}, and a comparative analysis was conducted on the fuel consumptions of the proposed hybrid electric propulsion system and the conventional mechanical propulsion system.

When the ship starts operating with an SOC_{batt} of 95%, Generator #1 and the battery manage the EL of the naval vessel, as shown in the left image of Figure 8. In section ①, which represents the departure preparation phase while docked, the initial EL is 149 kW, and in *S* mode, Generator #1 does not operate. This allows the battery with an SOC of 1508 kWh to manage the EL. Section ② represents the phase of moving to the mission area, where the ship transitions from low to high speed and the EL increases to a maximum of 9200 kW. When the EL is approximately 9150–9200 kW, Generator #1 operates in the 4-C mode as $\boldsymbol{DG_{opt}}$, while the battery alternates between charging and discharging to manage the EL. Section ③ refers to the phase of operating the unmanned underwater vehicle, during which the EL increases to a maximum of 9619 kW. When the EL is approximately 9600 kW, Generator #1 operates in the 4-F mode as $\boldsymbol{DG_{max}}$, while the battery alternates between charging and discharging to manage the EL. Section ④ pertains to the deep-sea rescue submersible phase, where the EL is approximately between 1550 and 1600 kW. In this scenario, Generator #1 operates in the 1-C mode as $\boldsymbol{DG_{max}}$, while SOC_{batt} is maintained at approximately 90%, effectively managing the EL. Sections ⑤, ⑦, and ⑨ correspond to phases where the vessel is in saturation diving waiting mode. During this period, the EL ranges between 1830 and 1910 kW. In this scenario, Generator #1 operates in the 1-C mode as $\boldsymbol{DG_{max}}$, while SOC_{batt} is maintained at approximately 90% to effectively manage the EL. Sections ⑥, ⑧, and ⑩ refer to periods when the vessel is engaged in saturation diving, with the EL increasing to a maximum of 9719 kW. Notably, during section ⑥, when SOC_{batt} is in the range of 90% > $SOC_{batt} \geq$ 20%, Generator #1 operates in the 4-F mode as $\boldsymbol{DG_{max}}$. However, in sections ⑧ and ⑩, when SOC_{batt} is 100% $\geq SOC_{batt}$ > 90%, Generator #1 operates in the 4-C mode as $\boldsymbol{DG_{opt}}$. Section ⑪ refers to the recovery operation phase, where the EL is approximately between 1393 and 1700 kW. During this time, Generator #1 operates in the 1-C mode as $\boldsymbol{DG_{max}}$, while SOC_{batt} is maintained at approximately 90%, effectively managing the EL. Section ⑫ describes the return phase to the base, during which the vessel travels at cruising speed. When the EL is approximately in the range of 4580 to 4670 kW, if SOC_{batt} is 100% $\geq SOC_{batt}$ > 90%, Generator #1 operates in the 2-A mode. If SOC_{batt} is 90% > $SOC_{batt} \geq$ 20%, the generator operates in the 2-D mode, with Generator #1 functioning in the $\boldsymbol{DG_{max}}$ mode.

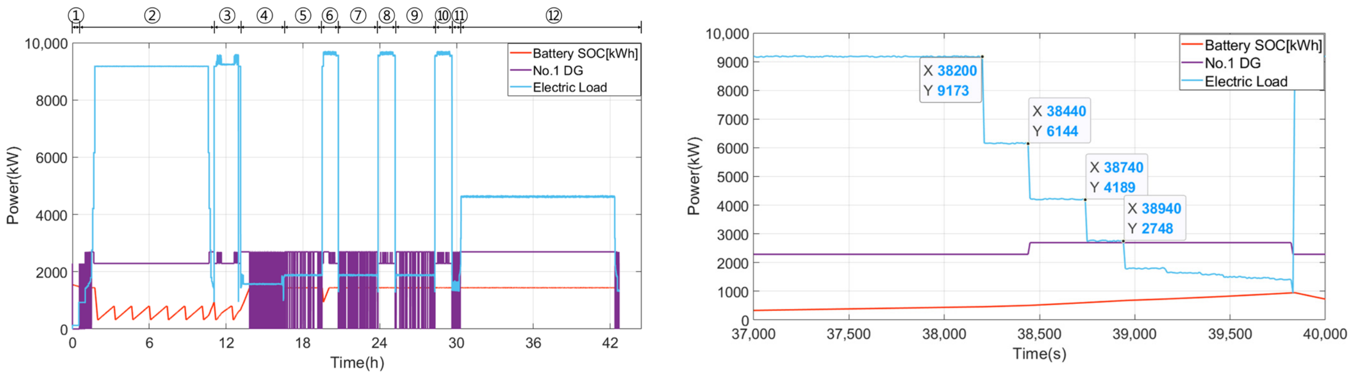

Figure 8. Simulation results for Generator #1.

As shown in the right diagram of Figure 8, during the time interval from 37,000 to 40,000 s in sections ② and ③, as the EL decreases from 9173 to 6144 kW, SOC_{batt} remains in the range of 90% > $SOC_{batt} \geq$ 20%. This condition prompts a transition from the 4-C to the 3-B mode, while Generator #1 maintains the $\boldsymbol{DG_{opt}}$ operating mode. As the EL decreases further from 6144 to 4189 kW, the SOC remains in the same range, resulting in a shift from the 3-B to the 2-D mode, with Generator #1 changing the operating mode from $\boldsymbol{DG_{opt}}$ to $\boldsymbol{DG_{max}}$. Finally, as the EL decreases from 4189 to 2748 kW, the SOC continues to fall within the same range, leading to a transition from the 2-D to the 2-A mode, while Generator #1 continues to operate in the $\boldsymbol{DG_{max}}$ mode.

When the vessel begins operating with an SOC_{batt} of 95%, Generator #2 and the battery manage the EL of the naval vessel, as depicted in the left diagram of Figure 9. In section ① (mooring and departure preparation phase), the initial EL is 149 kW, during which Generator #2 does not operate in the S mode, and the EL is managed solely by the battery (SOC = 1508 kWh). In section ②, when the EL is approximately 9150–9200 kW, Generator #2 operates in the 4-C mode under the $\boldsymbol{DG_{opt}}$ operational mode. In section ③, when the EL is approximately 9600 kW, Generator #2 switches to the 4-F mode in the $\boldsymbol{DG_{max}}$ operational mode. In section ④, when the EL is approximately 1550–1600 kW, Generator #2 does not operate in the 1-C mode. Similarly, in sections ⑤, ⑦, and ⑨, with ELs being approximately 1830 to 1910 kW, Generator #2 remains inactive in the 1-C mode. In section ⑥, when 90% > $SOC_{batt} \geq$ 20%, Generator #2 operates in the 4-F mode at the

$\boldsymbol{DG_{max}}$ operational mode. However, in sections ⑧ and ⑩, when 100% $\geq SOC_{batt} >$ 90%, Generator #2 operates in the 4-C mode under the $\boldsymbol{DG_{opt}}$ operational mode. In section ⑪, when the EL is about 1393 to 1700 kW, Generator #2 does not operate in the 1-C mode. Finally, in section ⑫, when the EL is approximately between 4580 and 4670 kW, if 100% $\geq$ $SOC_{batt} >$ 90%, Generator #2 operates in the 2-A mode under the $\boldsymbol{DG_{min}}$ operational mode; when 90% $> SOC_{batt} \geq$ 20%, the generator operates in the 2-D mode under the $\boldsymbol{DG_{max}}$ operational mode.

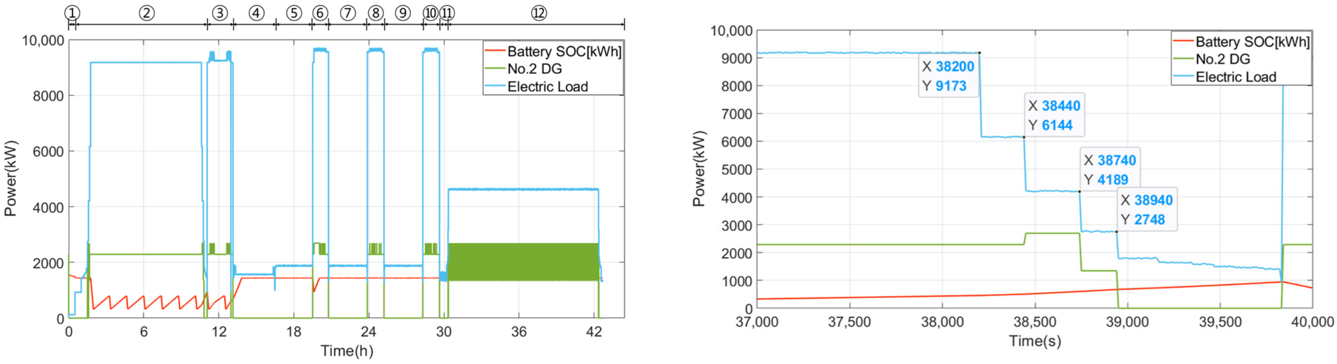

Figure 9. Simulation results for Generator #2.

As shown in the right diagram of Figure 9, during the time interval from 37,000 and 40,000 s for sections ② and ③, as the EL decreases from 9173 to 6144 kW, with 90% $> SOC_{batt} \geq$ 20%, the operation shifts from the 4-C to the 3-B mode, while Generator #2 maintains the $\boldsymbol{DG_{opt}}$ operational mode. When the EL drops from 6144 to 4189 kW, since 90% $> SOC_{batt} \geq$ 20%, the operation changes from the 3-B to the 2-D mode, and Generator #2 switches from the operational mode from DG_{opt} to $\boldsymbol{DG_{max}}$. As the EL further decreases from 4189 to 2748 kW, since 90% $> SOC_{batt} \geq$ 20%, the operation transitions from the 2-D to the 2-A mode, with Generator #2 operating in the $\boldsymbol{DG_{min}}$ operational mode.

When the ship begins operation with an SOC_{batt} of 95%, Generator #3 and the battery manage the EL of the naval ship, as shown in the left diagram of Figure 10. In section ① (departure preparation phase while docked), the initial EL is 149 kW. In this mode (*S* mode), Generator #3 does not operate, and the EL is managed solely by the battery with an SOC of 1508 kWh. In section ②, the EL is approximately 9150–9200 kW, Generator #3 operates in the 4-C mode under the $\boldsymbol{DG_{opt}}$ operational mode. In section ③, as the EL reaches approximately 9600 kW, Generator #3 shifts to the 4-F mode in the $\boldsymbol{DG_{max}}$ operational mode. In section ④, when the EL is approximately 1550–1600 kW, Generator #3 does not operate in the 1-C mode. Similarly, in sections ⑤, ⑦, and ⑨, Generator #3 does not operate in the 1-C mode when the EL is approximately between 1830 and 1910 kW. In section ⑥, when 90% $> SOC_{batt} \geq$ 20%, Generator #3 operates in the 4-F mode under the $\boldsymbol{DG_{max}}$ operational mode. In sections ⑧ and ⑩, when 100% $\geq SOC_{batt} >$ 90%, Generator #3 operates in the 4-C mode under the $\boldsymbol{DG_{opt}}$ operational mode. In Section ⑪, with the EL around 1393 to 1700 kW, Generator #3 does not operate in the 1-C mode. Finally, in section ⑫, when the EL is approximately 4580 to 4670 kW, if 100% $\geq SOC_{batt}$ >90%, Generator #3 operates in the 2-A mode; if 90% $> SOC_{batt} \geq$ 20%, it operates in the 2-D mode and Generator #3 is not operated.

As shown in the right figure of Figure 10, examining the interval between 37,000 and 40,000 s for sections ② and ③, the EL decreases from 9173 to 6144 kW. Since 90% $> SOC_{batt}$ $\geq$ 20%, the operation changes from the 4-C to the 3-B mode, while Generator #3 continues to operate in the $\boldsymbol{DG_{opt}}$ mode. When the EL decreases further from 6144 to 4189 kW, the operation transitions from the 3-B to the 2-D mode, and Generator #3 stops operating in the $\boldsymbol{DG_{opt}}$ operational mode. As the EL drops from 4189 to 2748 kW, the operation changes from the 2-D to the 2-A mode, with Generator #3 still not operating.

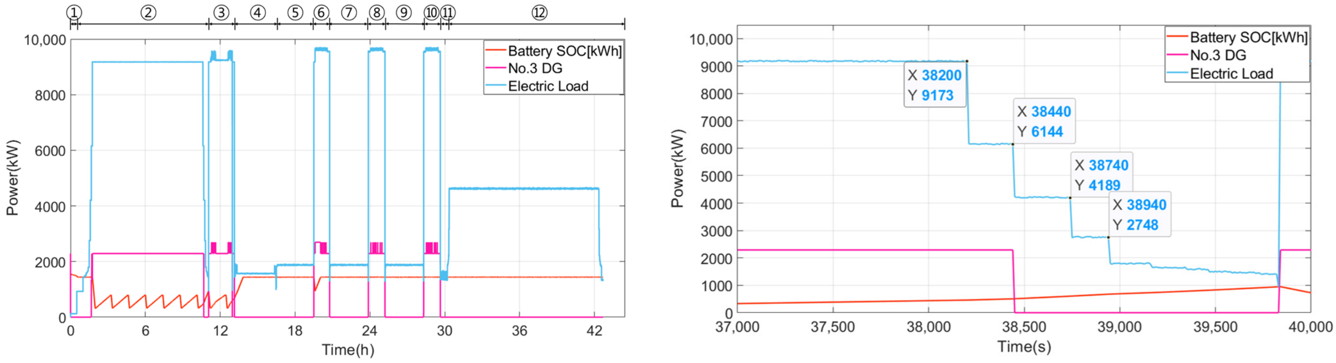

Figure 10. Simulation results for Generator #3.

When the ship begins its operation with an SOC_{batt} of 95%, Generator #4 and the battery manage the EL of the naval ship, as illustrated on the left side of Figure 11. In section ① (pre-departure period while the ship is docked), the initial EL is 149 kW. During this time, Generator #4 does not operate, and the EL is managed solely by the battery with an SOC of 1508 kWh. In section ②, as the EL reaches approximately 9150 to 9200 kW, Generator #4 operates in the 4-C mode under the $\boldsymbol{DG_{max}}$ operational mode. In section ③, as the EL approaches ~9600 kW, Generator #4 transitions to the 4-F mode, still under the $\boldsymbol{DG_{max}}$ operational mode. In section ④, when the EL is 1550–1600 kW, Generator #4 does not operate in the 1-C mode. Similarly, in sections ⑤, ⑦, and ⑨, Generator #4 does not operate in the 1-C mode when the EL is 1830–1910 kW. In section ⑥, when 90% > SOC_{batt} ≥ 20%, Generator #4 operates in the 4-F mode. In sections ⑧ and ⑩, when 100% ≥ SOC_{batt} > 90%, Generator #4 operates in the 4-C mode under the $\boldsymbol{DG_{max}}$ operational mode. In section ⑪, when the EL is 1393–1700 kW, Generator #4 does not operate in the 1-C mode. Finally, in section ⑫, when the EL is around 4580 to 4670 kW, if 100% ≥ SOC_{batt} > 90%, Generator #4 operates in the 2-A mode; if 90% > SOC_{batt} ≥ 20%, it operates in the 2-D mode and Generator #4 is not operated.

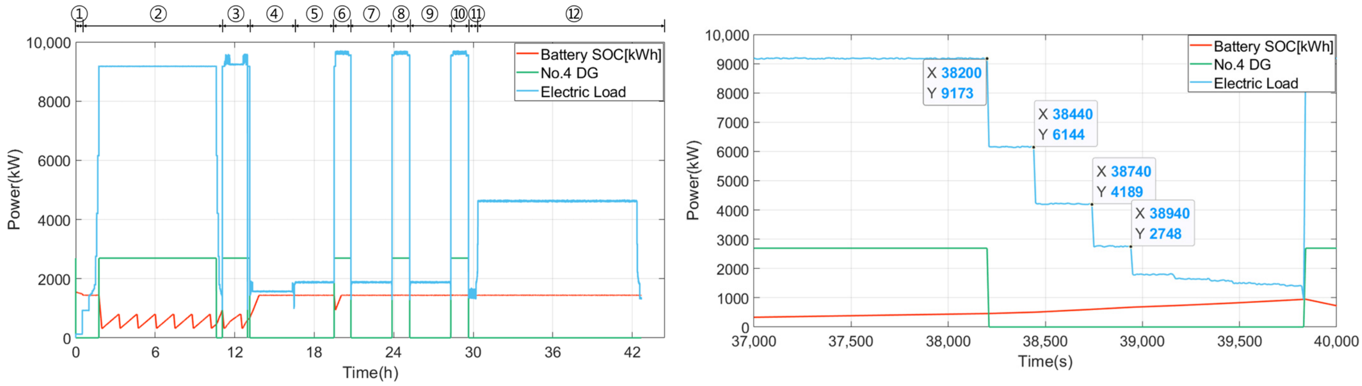

Figure 11. Simulation results for Generator #4.

As illustrated in the right figure of Figure 11, during the time interval from 37,000 and 40,000 s for sections ② and ③, the EL decreases from 9173 to 6144 kW. Since 90% > SOC_{batt} ≥ 20%, the operation changes from the 4-C to the 3-B mode, and Generator #4 ceases operation in the $\boldsymbol{DG_{max}}$ operational mode. As the EL continues to drop from 6144 to 4189 kW, the operation transitions from the 3-B to the 2-D mode, with Generator #4 not operating. Finally, as the EL decreases from 4189 to 2748 kW, the operation shifts from the 2-D to the 2-A mode, with Generator #4 still not operating.

The SFOC values per unit time were accumulated over the duration of the simulation to determine the total fuel consumption, as shown in Figure 12. The graph depicts the cumulative fuel consumption of each generator. At the end of the ~42 h simulation, the total cumulative fuel consumption for the four generators amounted to 41.5 tons. In contrast, the simulation of the existing mechanical propulsion system, based on the same load profile, resulted in a total fuel consumption of 53.4 tons. This comparison demonstrates that the proposed hybrid electric propulsion system achieves a fuel-saving effect of approximately 11.9 tons.

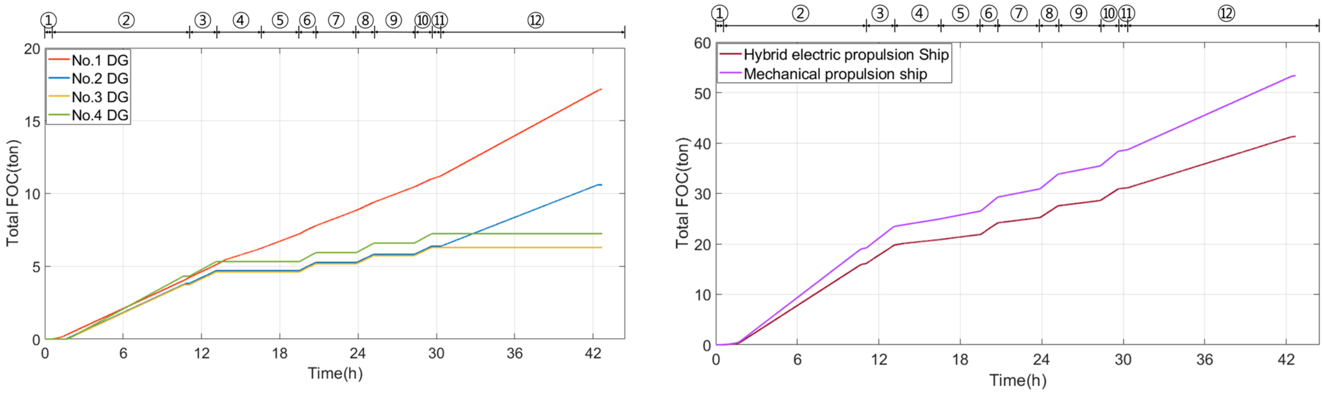

Figure 12. Comparation of total fuel oil consumption (FOC).

As shown in Table 13, Generator #1 is primarily operated, followed by Generator #2, while Generators #3 and #4 operate in a similar manner, contributing to the overall fuel consumption. The fuel consumption ratios of each generator compared with the total cumulative consumption were approximately 41.9% for Generator #1, 25.5% for Generator #2, 15.1% for Generator #3, and 17.3% for Generator #4.

Table 13. Total FOC of each generator.

No. 1 DG	No. 2 DG	No. 3 DG	No. 4 DG	Total
17.4	10.6	6.3	7.2	41.5

4. Discussion

4.1. Battery-Based Hybrid Electric System Design

To convert a naval vessel from a mechanical propulsion system into a hybrid electric propulsion system utilizing batteries, operational profile data were measured to design the power system. The total required power and propulsion load for the target vessel were confirmed to be between 960 and 9719 kW. By applying a margin of 1.15% based on the existing literature, four actual generator models were selected for the power system design. Furthermore, to determine the battery capacity, a battery with a capacity of 1600 kWh was chosen to meet the requirements related to the power supply during docking, low-speed navigation, and emergency situations. This operational profile-based design allowed for the optimization of the capacities of the diesel generators and batteries, suggesting that similar methods could be applied to the power system design of other vessels.

4.2. Validation of the Power Control System

To operate the diesel generators in their high-efficiency range, a control system was designed to ensure that individual diesel generators operate primarily in low-SFOC zones, with operational loads of 0%, 50%, 85%, and 100%. Additionally, based on the existing literature, battery safety was ensured by classifying batteries into three zones according to the SOC, with different operations for charging, discharging, and standby in each zone. A control matrix for the operating modes of the diesel units and batteries was constructed, and simulations were conducted using MATLAB/Simulink. The results confirmed that, consistent with the design intentions, the operating modes and load commands for the generators and batteries were effectively managed according to power load fluctuations, ensuring a stable system operation. The methods for designing control rules and logic for the operation of generators and batteries can be adapted to different vessel types, serving as a reference for future related research.

4.3. Comparison of FOC, Price, and Environmental Impact

As shown in Table 14, the simulation results, applying the proposed hybrid electric propulsion system to the target vessel's 42 h operating profile, demonstrated fuel savings of 12 tons compared with the existing mechanical propulsion system. This indicates that, while maintaining the same propulsion performance, fuel savings can effectively reduce operational costs and decrease carbon dioxide (CO_2) emissions stemming from the vessel's operation. By implementing a three-shift operation concept with the naval vessel's operational, standby, and maintenance periods (each lasting 4 months) and utilizing the analyzed 42 h operating profile for a total of 12 instances over the 4-month operational period (three times per month), an average annual fuel savings of 12 tons × 12 instances = 144 tons can be achieved. As shown in Table 14, this translates to annual savings of USD 86,688 in fuel costs and a reduction of 4.72 tons in CO_2 emissions.

Table 14. Savings in fuel costs and CO_2 reduction.

	Saving Cost	CO_2 Reduction
Savings of fuel per year [ton]	144	144
Low sulfur fuel oil USD per ton [USD] [47]	610	-
CO_2 emissions per ton * (distillate fuel oil [48])	-	0.03278123
Total	87,840 [USD]	4.72 [ton]

* For 1 US gallon of crude oil: convert to liters: 1 US gallon × 3.785 L/gallon = 3.785 L; convert to kilograms: 3.785 L × 0.85 kg/L = 3.217 kg; convert to tons: 3.217 kg/1000 = 0.003217 tons; CO_2 emissions per gallon to tons: 10.19 gallon [46] × 0.003217 ton/gallon = 0.03278123 ton.

This transition from a mechanical propulsion system to a battery-based hybrid electric propulsion system not only enhances efficiency but also provides significant environmental benefits. Additionally, it can lead to reduced costs, facilitating a more effective use of national tax resources.

4.4. Broader Implications and Applications

This study demonstrates the potential benefits of transitioning naval vessels to hybrid electric propulsion systems, including enhanced fuel efficiency, reduced carbon emissions, and significant cost savings. These findings suggest that similar hybridization strategies could be applied beyond naval vessels to various types of maritime vessels, such as commercial ships and passenger ferries. Additionally, incorporating renewable energy sources, such as solar or wind power, into the hybrid power system could further enhance the overall efficiency and environmental benefits. Future studies could explore the integration of renewable energy sources and examine the long-term reliability and maintenance challenges associated with hybrid electric propulsion systems, particularly in the harsh marine environment.

4.5. Policy and Strategic Considerations

The transition to battery-based hybrid electric propulsion systems for naval vessels also has important policy and strategic implications. By reducing dependency on traditional fossil fuels, naval operations can become more resilient against fuel supply disruptions and price fluctuations. This transition aligns with global decarbonization goals and could serve as a benchmark for future military and commercial vessel design. Moreover, hybrid systems could facilitate quieter operations, enhancing the tactical advantages of naval vessels in stealth missions. Further investigation into the policy impacts, cost–benefit analysis, and international standards for hybrid propulsion systems would provide a valuable framework for decision makers in the maritime sector.

4.6. Limitation and Future Research

In this study, a controller based on optimal operating points according to the load of the generators was successfully designed with a focus on minimizing fuel consumption, and the effectiveness of the hybrid electric propulsion system was validated through simulations using actual line data. However, it has the limitation that it has not been verified through real-world application on a ship. For the controller to be effectively implemented in real-world ship operations, it must consider transient states, including the operation, shutdown, and load fluctuations of the generators. Furthermore, to validate the performance of the hybrid propulsion system, it is necessary to assess the response of a more dynamic control system by applying various operational profiles and load conditions. However, in this study, modeling was conducted for simulations over a long timescale, and therefore, clear limitations exist in capturing these dynamic aspects. Additionally, when new operating modes are introduced or the system is expanded, more detailed designs and logical implementations are necessary. Nevertheless, when converting existing naval vessels to using hybrid electric propulsion systems for similar missions or when integrating this system into new naval vessels for mission execution, the power and control system design and verification techniques proposed in this study can be employed. Should such projects move forward, further research must be conducted as outlined above.

5. Conclusions

This study proposes a method for upgrading naval vessels with traditional mechanical propulsion systems into a hybrid electric propulsion system that utilizes batteries. By evaluating the advantages and disadvantages of different types of ship propulsion systems, the superiority of hybrid electric propulsion systems was confirmed, emphasizing the need for their adoption. In addition, through an examination of power management techniques from existing electric propulsion systems and an analysis of the power loads required by naval vessels (alongside battery power capacity), a system was designed to ensure that the generators operate in high-efficiency modes. The key findings are as follows:

1. To transition naval vessels with traditional mechanical propulsion systems to hybrid propulsion systems that utilize batteries, the specifications of the generators and batteries were appropriately selected. Considering the maximum power load required by the target vessel, which was calculated at 9719 kW (based on the power load of the equipment operated according to the ship's mission), four diesel generators with a capacity of 2693 kW were chosen, incorporating a safety margin of 15%. Additionally, a battery with a capacity of 1600 kWh was selected to meet the power supply requirements during docking, low-speed navigation, and emergency situations and ensure SOC safety, thus enabling the design of the overall power system.
2. Through a review of the existing literature, SOC_{batt} was designed as follows: the range of 100% $\geq SOC_{batt} \geq$ 90% indicates battery charging, 90% > $SOC_{batt} \geq$ 20% allows for either battery charging or discharging, and 20% > $SOC_{batt} \geq$ 0% facilitates discharging. The generators were set (according to the EL) to operate in the following modes: DG_{stop} (EL: 0%), DG_{min} (EL: 50%), DG_{opt} (EL: 85%), and DG_{max} (EL: 100%). This resulted in the design of 20 operational modes based on different combinations of generator modes. It was confirmed that the system operated in 23 operational modes, depending on the EL and battery SOC. The corresponding controller was modeled in MATLAB/Simulink and applied to the power system, where real operating data were input for the simulation, confirming that the system functioned as intended.
3. Based on the operational modes of the target naval vessel, the collected propulsion and power profiles were simulated in MATLAB/Simulink for both the existing mechanical propulsion system and the proposed hybrid electric propulsion system. The results showed that the total fuel consumption was 53.4 tons for the existing mechanical

propulsion system and 41.5 tons for the proposed hybrid electric propulsion system, confirming that the proposed hybrid electric propulsion system achieves a fuel saving of ~11.9 tons, representing a reduction of 22%.

4. Finally, the economic benefits of fuel savings (obtained from the simulation) and the reduced CO_2 emissions were discussed. By applying the typical operational concept of Republic of Korea Navy vessels and adjusting the annual operating hours, it was found that the battery-based hybrid electric propulsion vessels achieve an annual fuel savings of 144 tons compared with the mechanical propulsion system. This results in an annual fuel cost savings of USD 86,688 and a reduction of 4.72 tons in CO_2 emissions.

Author Contributions: Conceptualization, Y.P.; methodology, Y.P.; software, H.K.; validation, H.K.; formal analysis, Y.P. and H.K.; investigation, Y.P. and H.K.; resources, Y.P.; data curation, Y.P.; writing—original draft, Y.P.; writing—review and editing, H.K.; visualization, Y.P.; supervision, H.K.; project administration, H.K.; funding acquisition, H.K. All authors have read and agreed to the published version of the manuscript.

Funding: This research was supported by the Korea Planning and Evaluation Institute of Industrial Technology (KEIT) funded by the Ministry of Commerce, Industry, and Energy (RS-2022-00144151).

Institutional Review Board Statement: Not applicable.

Informed Consent Statement: Not applicable.

Data Availability Statement: Data presented in this article are available upon request from the corresponding authors.

Conflicts of Interest: The authors declare no conflicts of interest.

Abbreviations

Battery state 1: battery-only charging mode; Battery state 2: battery charging and discharging mode; Battery state 3: battery-only discharging mode; CODLOG: combined diesel-electric or gas turbine; CODLOD: combined diesel-electric or diesel engine; COGAG: combined gas and gas; CODAG: combined diesel or gas; CODAD: combined diesel or diesel; DP: dynamic programming; EMS: energy management system; EL: electrical load; ECMS: equivalent consumption minimization strategy; HEV: hybrid electric vehicle; IPES: integrated power and energy system; MPC: model predictive control; PMS: power management system; SFOC: specific fuel oil consumption; SOC: battery state of charge.

References

1. Richardson, J.M. *Naval Power and Energy Systems, Technology Development Roadmap (US Navy Power and Energy Leap Forward)*; Naval Sea Systems Command; U.S. Naval: Arlington, VA, USA, 2019.
2. Technology, N. Type 23 Duke Class Frigate. Available online: https://www.naval-technology.com/projects/t23/ (accessed on 7 September 2024).
3. Vernova, G. Integrated Electrical Propulsion System for US Navy DDG 1000 Destroyers. Available online: https://www.gevernova.com (accessed on 7 September 2024).
4. Shin, S.; Park, J.; Yong, Y.; Oh, K. Propulsion System of ROKN Warships & Future of Propulsion System. *J. Korean Soc. Propuls. Eng.* **2021**, *25*, 53–59.
5. Marine Battery Market to Surpass USD 2304.59 Million by 2031: SkyQuest Technology. Available online: https://www.globenewswire.com (accessed on 4 November 2024).
6. Geertsma, R.; Negenborn, R.; Visser, K.; Hopman, J. Design and control of hybrid power and propulsion systems for smart ships: A review of developments. *Appl. Energy* **2017**, *194*, 30–54. [CrossRef]
7. Carlton, J. *Marine Propellers and Propulsion*; Butterworth-Heinemann: Oxford, UK, 2018.
8. Baldi, F.; Johnson, H.; Gabrielii, C.; Andersson, K. Energy and exergy analysis of ship energy systems–the case study of a chemical tanker. *Int. J. Thermodyn.* **2015**, *18*, 82–93. [CrossRef]
9. Dzida, M. On the possible increasing of efficiency of ship power plant with the system combined of marine diesel engine, gas turbine and steam turbine, at the main engine-steam turbine mode of cooperation. *Pol. Marit. Res.* **2009**, *16*, 47–52. [CrossRef]
10. Sáiz, V.M.M.; López, A.P. Future trends in electric propulsion systems for commercial vessels. *J. Marit. Res.* **2007**, *4*, 81–100.

11. Prenc, R.; Cuculić, A.; Baumgartner, I. Advantages of using a DC power system on board ship. *Pomor. Zb.* **2016**, *52*, 83–97. [CrossRef]
12. Mashayekh, S.; Wang, Z.; Qi, L.; Lindtjorn, J.; Myklebust, T.-A. Optimum sizing of energy storage for an electric ferry ship. In Proceedings of the 2012 IEEE Power and Energy Society General Meeting, San Diego, CA, USA, 22–26 July 2012; pp. 1–8.
13. Van Biert, L.; Godjevac, M.; Visser, K.; Aravind, P.V. A review of fuel cell systems for maritime applications. *J. Power Sources* **2016**, *327*, 345–364. [CrossRef]
14. Bayraktar, M.; Cerit, G. An assessment on the efficient use of hybrid propulsion system in marine vessels. *World J. Environ. Res.* **2020**, *10*, 61–74. [CrossRef]
15. Gully, B.H. Hybrid Powertrain Performance Analysis for Naval and Commercial Ocean-Going Vessels. Ph.D. Thesis, The University of Texas at Austin, Austin, TX, USA, 2012.
16. Buckingham, J. Hybrid drives for naval auxiliary vessels. In Proceedings of the Pacific International Maritime Conference, Sydney, Australia, 7–9 October 2013.
17. Castles, G.; Reed, G.; Bendre, A.; Pitsch, R. Economic benefits of hybrid drive propulsion for naval ships. In Proceedings of the 2009 IEEE Electric Ship Technologies Symposium, Baltimore, MD, USA, 20–22 April 2009; pp. 515–520.
18. Trovão, J.P.; Machado, F.; Pereirinha, P.G. Hybrid electric excursion ships power supply system based on a multiple energy storage system. *IET Electr. Syst. Transp.* **2016**, *6*, 190–201. [CrossRef]
19. Dedes, E.K.; Hudson, D.A.; Turnock, S.R. Assessing the potential of hybrid energy technology to reduce exhaust emissions from global shipping. *Energy Policy* **2012**, *40*, 204–218. [CrossRef]
20. Sui, C.; de Vos, P.; Stapersma, D.; Visser, K.; Ding, Y. Fuel consumption and emissions of ocean-going cargo ship with hybrid propulsion and different fuels over voyage. *J. Mar. Sci. Eng.* **2020**, *8*, 588. [CrossRef]
21. Register, K. *Guidance for DC Distribution Systems*; Korea Register: Busan, Republic of Korea, 2023.
22. Liao, W.; Dong, X.; Yang, R.; Qiao, Z. Control Optimization Method for Ship Direct Current Microgrid Based on Impedance Reshaping. *J. Mar. Sci. Eng.* **2024**, *12*, 503. [CrossRef]
23. Farhadi Gharibeh, H.; Farrokhifar, M. Online multi-level energy management strategy based on rule-based and optimization-based approaches for fuel cell hybrid electric vehicles. *Appl. Sci.* **2021**, *11*, 3849. [CrossRef]
24. Peng, X.; Chen, H.; Guan, C. Energy management optimization of fuel cell hybrid ship based on particle swarm optimization algorithm. *Energies* **2023**, *16*, 1373. [CrossRef]
25. Kim, K.-I.; Lee, K.M. Dynamic programming-based vessel speed adjustment for energy saving and emission reduction. *Energies* **2018**, *11*, 1273. [CrossRef]
26. Marín, L.G.; Sumner, M.; Muñoz-Carpintero, D.; Köbrich, D.; Pholboon, S.; Sáez, D.; Núñez, A. Hierarchical energy management system for microgrid operation based on robust model predictive control. *Energies* **2019**, *12*, 4453. [CrossRef]
27. Gao, D.; Jiang, H.; Shi, W.; Wang, T.; Wang, Y. Adaptive equivalent consumption minimization strategy for hybrid electric ship. *Energy Sci. Eng.* **2022**, *10*, 840–852. [CrossRef]
28. Chua, L.W.Y. A Strategy for Power Management of Electric Hybrid Marine Power Systems. Ph.D. Thesis, Nanyang Technological University, Singapore, 2019.
29. Zhaoxia, X.; Tianli, Z.; Huaimin, L.; Guerrero, J.M.; Su, C.-L.; Vásquez, J.C. Coordinated control of a hybrid-electric-ferry shipboard microgrid. *IEEE Trans. Transp. Electrif.* **2019**, *5*, 828–839. [CrossRef]
30. Roslan, S.B.; Tay, Z.Y.; Konovessis, D.; Ang, J.H.; Menon, N.V. Rule-based control studies of LNG–battery hybrid tugboat. *J. Mar. Sci. Eng.* **2023**, *11*, 1307. [CrossRef]
31. Karim, N.; Lisner, R.; Kazemi, H.; Annaz, F. Rule-based power management for the all-electric ship. In Proceedings of the Australian University Power Engineering Conference, Melbourne, Australia, 29 September–3 October 2002.
32. Tang, D.; Yan, X.; Yuan, Y.; Wang, K.; Qiu, L. Multi-agent based power and energy management system for hybrid ships. In Proceedings of the 2015 International Conference on Renewable Energy Research and Applications (ICRERA), Palermo, Italy, 22–25 November 2015; pp. 383–387.
33. La Tona, G.; Luna, M.; di Piazza, M.C.; Pietra, A. Energy management system for efficiency increase in cruise ship microgrids. In Proceedings of the IECON 2019-45th Annual Conference of the IEEE Industrial Electronics Society, Lisbon, Portugal, 14–17 October 2019; pp. 4056–4062.
34. Haseltalab, A.; Negenborn, R.R. Model predictive maneuvering control and energy management for all-electric autonomous ships. *Appl. Energy* **2019**, *251*, 113308. [CrossRef]
35. Wang, Z.; Ma, Y.; Sun, Y.; Tang, H.; Cao, M.; Xia, R.; Han, F. Optimizing energy management and case study of multi-energy coupled supply for green ships. *J. Mar. Sci. Eng.* **2023**, *11*, 1286. [CrossRef]
36. Bellman, R.; Kalaba, R.E. *Dynamic Programming and Modern Control Theory*; Citeseer: Cambridge, MA, USA, 1965; Volume 81.
37. Vinot, E. Time reduction of the dynamic programming computation in the case of hybrid vehicle. *Int. J. Appl. Electromagn. Mech.* **2017**, *53*, S213–S227. [CrossRef]
38. Panday, A.; Bansal, H.O. A review of optimal energy management strategies for hybrid electric vehicle. *Int. J. Veh. Technol.* **2014**, *2014*, 160510. [CrossRef]
39. Wirasingha, S.G.; Emadi, A. Classification and review of control strategies for plug-in hybrid electric vehicles. *IEEE Trans. Veh. Technol.* **2010**, *60*, 111–122. [CrossRef]

40. Sultana, W.R.; Sahoo, S.K.; Sukchai, S.; Yamuna, S.; Venkatesh, D. A review on state of art development of model predictive control for renewable energy applications. *Renew. Sustain. Energy Rev.* **2017**, *76*, 391–406. [CrossRef]
41. Ge, Y.; Zhang, J.; Zhou, K.; Zhu, J.; Wang, Y. Research on energy management for ship hybrid power system based on adaptive equivalent consumption minimization strategy. *J. Mar. Sci. Eng.* **2023**, *11*, 1271. [CrossRef]
42. Kalikatzarakis, M.; Geertsma, R.; Boonen, E.; Visser, K.; Negenborn, R. Ship energy management for hybrid propulsion and power supply with shore charging. *Control Eng. Pract.* **2018**, *76*, 133–154. [CrossRef]
43. ASR-21. ROKS Cheonghaejin. Available online: https://en.wikipedia.org/wiki/ROKS_Cheonghaejin_(ASR-21) (accessed on 18 September 2024).
44. Pham, V.C.; Kim, H.; Choi, J.-H.; Nyongesa, A.J.; Kim, J.; Jeon, H.; Lee, W.-J. Effectiveness of the Speed Reduction Strategy on Exhaust Emissions and Fuel Oil Consumption of a Marine Generator Engine for DC Grid Ships. *J. Mar. Sci. Eng.* **2022**, *10*, 979. [CrossRef]
45. Kolodziejski, M.; Michalska-Pozoga, I. Battery energy storage systems in ships' hybrid/electric propulsion systems. *Energies* **2023**, *16*, 1122. [CrossRef]
46. Peralta, P.; César, O.; Vieira, G.T.; Meunier, S.; Vale, R.J.; Salles, M.B.; Carmo, B.S. Evaluation of the CO_2 emissions reduction potential of Li-ion batteries in ship power systems. *Energies* **2019**, *12*, 375. [CrossRef]
47. Ship&Bunker. World Bunker Prices. World Bunker Prices—Ship&Bunker. Available online: https://shipandbunker.com (accessed on 7 September 2024).
48. U.S. Energy Information Administration. Carbon Dioxide Emissions Coefficients. U.S. Energy Information Administration—EIA—Independent Statistics and Analysis. Available online: https://www.eia.gov/ (accessed on 7 September 2024).

Disclaimer/Publisher's Note: The statements, opinions and data contained in all publications are solely those of the individual author(s) and contributor(s) and not of MDPI and/or the editor(s). MDPI and/or the editor(s) disclaim responsibility for any injury to people or property resulting from any ideas, methods, instructions or products referred to in the content.